ADDIS ABABA UNIVERSITY
SCHOOL OF GRADUATE STUDIES

PHOTOVOLTAIC PROPERTIES OF POLY[3-(4-OCTYLPHENYL)-2,2'-BITHIOPHENE] (PTOPT)

TOLESSA YADETE

JUNE 1998

Photovoltaic Properties of Poly[3-(4-Octylphenyl)-2,2'-Bithiophene] (PTOPT)

A Thesis

Submitted to the

School of Graduate Studies

Addis Ababa University

In Partial Fulfillment

of the Requirements for the Degree

of Master of Science in

Physics

By

Tolessa Yadete

June 1998

Addis Ababa

ADDIS ABABA UNIVERSITY

SCHOOL OF GRADUATE STUDIES

PHOTOVOLTAIC PROPERTIES OF POLY[3-(4-OCTYLPHENYL)-2,2'-BITHIOPHENE] (PTOPT)

By

Tolessa Yadete

Department of Physics

Faculty of Science

Addis Ababa University

APPROVED BY THE EXAMINATION COMMITTEE

Dr. Bantikassegn Workalemahu _____

Advisor

Dr. Ulrich Stutenbaeumer _____

Examiner

Prof. S. K. Sharma _____

Examiner

To the memory of

my father Yadete Bedane

and

my brother Dadi Yadete

Acknowledgment

I am highly indebted to my advisor, Dr. Bantikassegn Workalemahu for helping me to do my research in the field of conducting polymer physics, his excellent guidance, encouragement , invaluable and limitless effort with full patience in supervising this work. The convenient working environment he has created with the necessary materials including personal computer is greatly appreciated.

I wish to acknowledge the staffs of Physics Department for their support and encouragement. In particular, I am especially indebted to Dr. Fesseha Kassahun for his sustained support in the course of my study.

I am also thankful to Associate prof. Bernd Hundhammer, who has given me some of the articles on conducting polymers and also allow me to use his personal computer for the drawing of the chemical structures of conjugated polymers used in this work.

Special thanks are due to Oromia Educational Bureau for the sponsorship they granted me to participate in the graduate program.

I would like to express my sincere thanks to my friends in Fitche and Addis Ababa, too numerous to mention individually, who have helped and encouraged me during my stay at Addis Ababa University. I would particularly like to thank Ato Merga Kebede, Ato Getachew Negash, Dr. Minyishu Zewudie, Ato Tefera Tadesse, Engineer Berhanu Zewudie, for their material support and encouragement during my study.

My brothers; Ketema, Regassa, and Tafa Yadete and my sisters; Worki and Lomi Yadete, and Zinash Ababu deserve my deepest appreciation for their constant support and moral encouragement throughout my study.

Contents

List of tables

Table

List of Figures

Figure

Abstract

The purpose of this study is to investigate the photovoltaic effect of the undoped poly[3-(4-octylphenyl)-2,2'-bithiophene] (PTOPT) by performing the current density-voltage (J-V) measurements in the dark and under illumination. The Al/PTOPT junction forms a Schottky barrier. The semiconductor property of PTOPT was confirmed from optical absorption spectroscopy. The electrical and photovoltaic properties of an Al/PTOPT/ITO device were investigated by the J-V measurement in the dark and under illumination. From J-V in the dark, the reverse saturation current density, $J_0 = 6.7 \times 10^{-14} A/cm^2$ was obtained. The diode ideality factor n and the barrier height Φ_b are 4.0 and 1.2V, respectively. Optical absorption reveals that the band gap, E_g, of PTOPT is about 2.0eV. From photovoltaic characterization, the open-circuit voltage and the short-circuit current density of the device are $V_{oc} = 0.75V$ and $J_{sc} = 2.5 \times 10^{-5} A/cm^2$, respectively. The effective area of the cell was 0.06cm^2. The fill-factor and the power conversion efficiency obtained was 0.2 and 0.004% respectively. The illumination of the sample was made from the ITO side with a white light of intensity about 100mW/cm^2.

1 INTRODUCTION

A huge amount of research and technological application of solar energy utilization is carried out in converting light energy from the sun to electrical energy. The most important application of photovoltaic energy conversion in the past has been in space program. To day, however, the rising price of the fuel, the realization that oil and gas supplies can only last a relatively few decades, and the freedom of solar energy from pollution, have all led to closer looks at solar energy as an alternative to present day fossil-fuel system [1].

The silicon solar cell was first developed by Chapin, Fuller, and Pearson in 1954 using a diffused silicon p-n junction [2]. Since then the development of solar cell technology has grown considerably. Quit a number of research and development work on the use of solar cells has been made using inorganic semiconductors as photovoltaic materials. There has been also a new research work which uses organic polymers as active materials in the electronic and photovoltaic applications. Photovoltaic effects of conjugated polymers have been studied using a metal/polymer/metal device configuration. Interest in the study of conducting polymers arose because of the advantage they offer over the conventional inorganic semiconductors. They are potentially inexpensive, and readily available. The actual fabrication of the devices can be rather simple and low cost compared with the techniques presently used in most inorganic systems. For example, samples can be prepared using a well known spin coating and vacuum deposition techniques which are easy. Since many of polymeric materials can be used in thin-film forms as a result material costs can be reduced considerably [3]. The uses of conducting polymers is not limited to only photovoltaic applications, but also they are studied for a wide variety of uses in the integrated circuits, lightweight battery components, sensors,

electrochromic displays, light emitting diodes, lightweight wiring, and for other electronic and optoelectronic devices.

Schottky barrier solar cells based on the metal-polymer junction is one of the device structures in which photovoltaic properties of the polymers is studied. The main objective of this work is to characterize the electrical and photovoltaic properties of the device made from conjugated polymer, poly[3-(4-octylphenyl)-2,2'-bithiophene], (PTOPT), and consequently, to observe the photovoltaic energy conversion possibility of this device. This work is limited only to the investigation of the photovoltaic effect of the device.

Chapter 2 presents the concept of hybridization in the formation of molecular orbital using H-H and C-H bonds in ethylene, methane, and acetylene compounds. The chapter includes illustration of the formation of valence band and conduction band in conjugated polymers.

Chapter 3 treats the electrical properties of conducting polymers by explaining the possibility of varying their electrical conductivity over the full range from insulator to semiconductor and metal, through doping chemically or electrochemically. The special nature of charge carriers in conjugated polymers, the concept of solitons in degenerate ground state and polarons and bipolarons in non-degenerate ground state conducting polymers have been discussed. Different conductivity models that have been proposed to explain the conductivity of polymers are also included. Finally, the electrical properties of Schottky barrier junctions and ohmic contacts are presented.

Chapter 4 presents the physics of photovoltaic devices, and chapter 5 describes the experimental apparatus that are used in this work with the procedures for operating them. Chapter 6 provides the results obtained and the discussion of the results. At last the concluding remarks have been given in chapter 7.

2 SEMICONDUCTING ORGANIC POLYMERS

Research in the field of conducting polymers indicate that the electrical properties of conjugated polymers are similar to those of conventional inorganic semiconductors. They offer a viable alternative to the conventional inorganic semiconductors in many applications because of their unusual electrical properties, diversity, ease of device fabrication, large area and low cost [4].

The prospect of applications of organic semiconductors in the areas of sensors, batteries, micromuscles, large screen displays, electronic and optoelectronic devices, etc., has triggered considerable research activity and it offers a wealth of opportunities to develop exciting new products for the next few decades.

Undoped or/and doped conjugated polymers, such as polypyrrole [4] polyaniline [5] and polythiophenes and its derivatives [6, 7, 8] have shown semiconducting behavior that can be used in electronic and optoelectronic device applications. For instance the rectifying behavior of undoped poly[3-(4-octylphenyl)-2,2'-bithiophene], (PTOPT), [7] indicates that it can be used in photovoltaic device fabrication. In this work the photovoltaic and electrical properties of the Al/PTOPT/ITO sandwich structure will be studied.

2.1 WHAT ARE POLYMERS?

The term polymer is defined as a substance composed of a very large molecule (macro molecule). It is made up of small fundamental repeating unit called monomer. Polymers can consist of 10^5 to 10^6 (or even greater) number of monomers linked together with covalent bonds to form a macromolecular chain. The term polymer includes synthetic and natural macromolecules. Synthetic polymers are produced in a laboratory under controlled conditions. Polymers made from only one type of monomer units is called homopolymer,

where as a copolymer contains structural units of two or more different precursors. Polymers can also be classified as linear, branched, or cross linked. The cross-linked polymers have three-dimensional network structure and because of this they are stiff and durable.

An example of a linear polymer is polyacetylene whose electrical properties are extensively studied. PTOPT and PDOPT are examples of branched polymers. Mechanical and electrical properties of a polymer depend on such characteristics of macromolecules. As far as the electrical properties are concerned, the effect of cross-linking is to lower the conductivity. Polymers can exist as amorphous, or a mixture of crystalline and amorphous material. Even highly crystalline polymers contain a considerable amorphous portion [3]. Conducting polymers are semi-crystallized.

2.2 Chemical Bonding and Molecular Orbital Theory

2.2.1 Sigma (σ) and pi (π) bonds

Organic polymers are formed as a result of the covalent bond which holds different atoms together. Most polymers are covalently bonded long chain macromolecules. To understand the nature of the physical and electrical properties of the polymers one needs to know the structure of polymers and hence the nature of covalent bonds in polymers.

Covalent bonds are formed much in the same way in which two hydrogen atoms form a hydrogen molecule. Quantum Mechanics shows that wave function of chemical bond is derived from the combination of hydrogen like wave functions for the two atoms. By the linear combination of atomic orbital (LCAO) we have the new wave function which results in constructive combination of atomic orbitals and increase electron probability between the nuclei and leads to energetically favourable bonding molecular orbital (MO). The anti-bonding molecular orbital resulting from a destructive interaction has a region of zero

electron probability between the nuclei [9]. When a pair of atomic orbital is combined, a molecular orbital is produced.

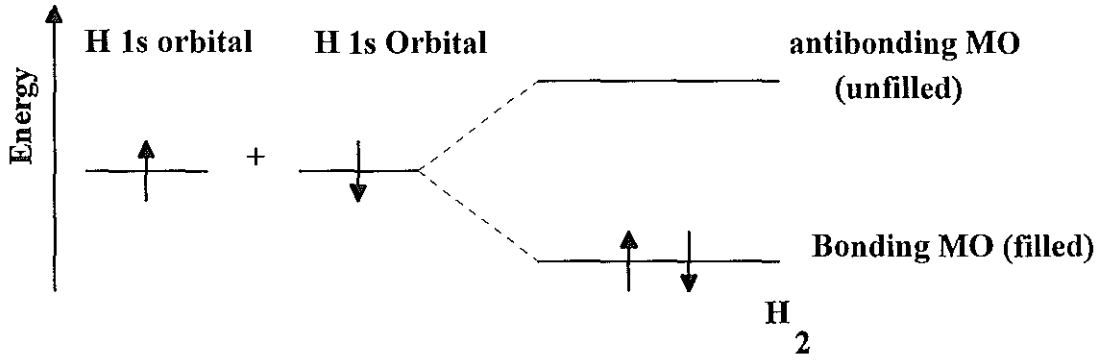

Fig. 2.1 Formation of bonding and antibonding orbitals as a result of linear combination of atomic orbitals (LCAO).

The bonding of MO in a hydrogen molecule has an orbital that is cylindrically symmetrical about the internuclear axis. Such bonds are known as sigma (σ) bonds. The antibonding molecular orbital that corresponds to σ-bonding MO is called σ* molecular orbital. Two different kinds of atomic orbitals can also combine to produce the molecular orbital of σ-bond. For example, 1s and 2p atomic orbitals lead to a molecular orbital of some what different shapes that are formed by two 1s or two 2p atomic orbitals.

Another type of bonding by which the two atomic orbitals can interact is π-bonding molecular orbital. Side-to-side interaction of p orbitals as shown in the Fig. 2.2b leads to a bonding that is not cylindrically symmetrical about the line joining the two nuclei. Such bonding of MO is called pi (π) MO and the associated antibonding is called the pi-star (π^*) molecular orbital. Hence, bonds of organic molecules are combinations of a sigma and one or more π-bonds.

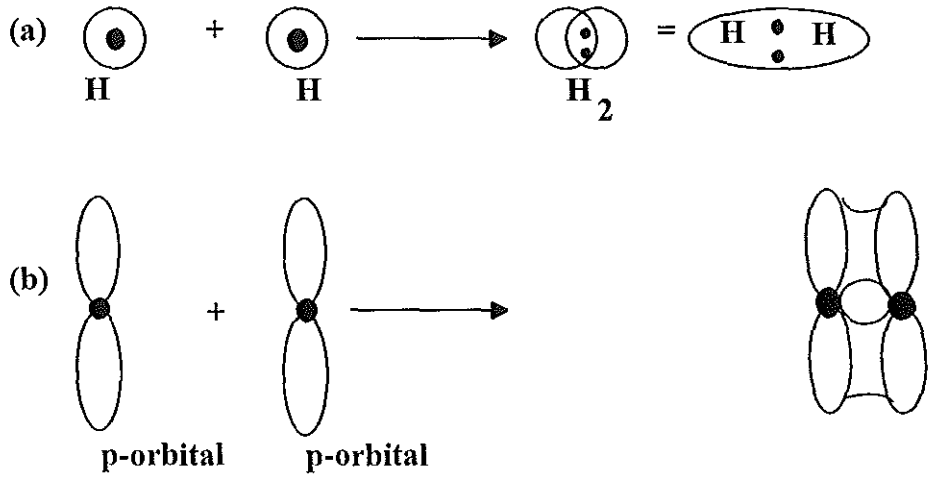

Fig. 2.2 Formation of σ-bonds and π-bonds by overlap of s orbitals (a) and p orbitals (b).

2.2.2 Hybridization

The concept of hybridization of atomic orbitals explains how, for example, carbon forms four equivalent tetrahedron bonds with hydrogen in methane. The ground state electronic configuration of a carbon atom is $1s^2 2s^2 2p^1_x 2p^1_y 2p^0_z$. The outer shell has four electrons, two of which are paired in the 2s orbital, and two are unpaired and occupy different 2p orbitals. To form four bonds, a carbon atom can adopt an electronic configuration different from the ground state configuration by promoting one electron from 2s orbital into the vacant $2p_z$ orbital, and achieve an excited state configuration $1s^2 2s^1 2p^1_x 2p^1_y 2p^1_z$. The combination of an s orbital and three p orbitals can be mixed or hybridized to form four equivalent new atomic orbitals that are spatially oriented towards the corners of the tetrahedron in CH_4. The new tetrahedral orbitals are called sp^3 hybrids, since they are constructed from one 2s orbital and three 2p orbitals.

In methane the sp^3 hybrid orbitals overlap with 1s atomic orbitals of four hydrogen atoms to form four σ-bond MOs. It has four bonding MO which are filled.

Another type of hybridization is an sp^2 hybrid orbital which is used in the formation of the structure of ethylene. Here a combination of 2s orbital with two of the three available 2p orbitals, the sp^2 hybrid orbitals, results and one unhybridized 2p orbital remains unchanged. The three sp^2 orbitals lie in a plane at an angles of 120° to each other, and the remaining p orbital is perpendicular to the sp^2 plane. In ethylene (C_2H_4) sp^2 hybridized carbons with another sp^2 hybridized carbon forms a strong σ-bond by sp^2-sp^2 overlap. When this occurs the unhybridized p orbitals on each carbon also approach each other in the correct geometry side ways over lap to form a π-bond. The combination of sp^2-sp^2 σ over lap and 2p-2p π-overlap results in the formation of a carbon-carbon double bond. In the complete structure of ethylene, overlap of two sp^2 hybrid orbitals and 1s atomic orbitals of hydrogen atoms form four σ- bond (Fig. 2.3) [10].

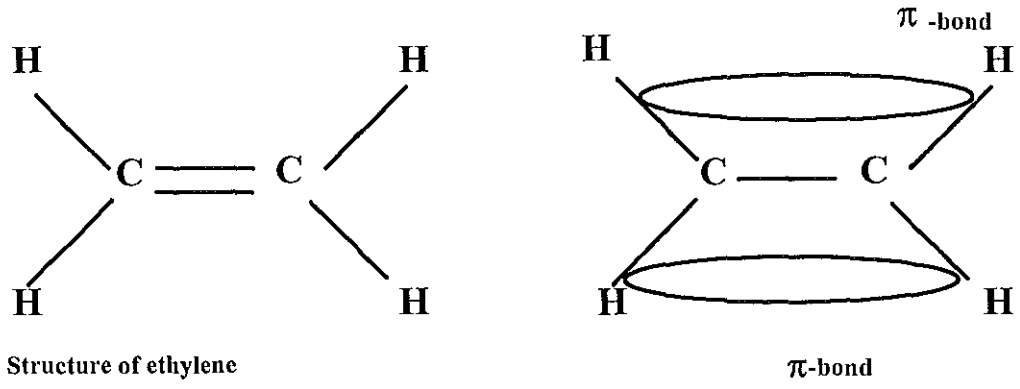

Fig. 2.3 Formation of π-bond as a result of 2p orbitals overlap.

The sp orbital hybridization is a different type of hybridization which is used in the formation of acetylene (C_2H_2). Acetylene is formed by a carbon-carbon triple bond. In this case the carbon 2s orbital hybridizes with only a single p orbital, and two sp hybridized

orbitals result, and two p orbitals remain unchanged. These sp orbitals are linear. They are 180^0 apart on the x-axis . The remaining two p orbitals are on the y-axis and z-axis. If two sp hybridized carbon atoms approach each other, sp orbitals from each carbon atom overlap head-on to form an sp-sp sigma bond. In addition, the p_y orbitals from each carbon atom form a p_y-p_y π-bond by overlapping side ways and the two p_z orbitals similarly overlap to form a p_z-p_z π-bond. As a result, a carbon-carbon triple bond is formed from these, one σ-bond and two π-bonds. The remaining sp hybrid orbitals form sigma bond to hydrogen 1s orbitals to complete the acetylene molecule (Fig. 2.4).

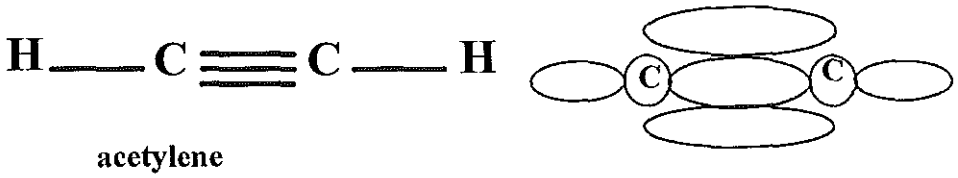

acetylene

Fig. 2.4 A carbon-carbon triple bond in acetylene.

The formation of a π-bond in organic materials gives rise to electron delocalization and builds up what is called the delocalized π-electron system. The structures of polymers and their properties are influenced by the nature of hybridization. Organic polymers may be formed by localized σ-bond orbital hybridization and delocalized π-bond. In those formed by σ-bonds only, the separation between bonding (HOMO - highest occupied MO, or valence band) and antibonding (LUMO - Lowest Unoccupied MO, or conduction band) is large so that the band gap energy (E_g) is large. On the other hand those organic polymers which have π-bonds in addition to σ-bonds, (e.g. sp^2 hybridization) yields smaller separation between the bonding (π) and antibonding (π^*) states and hence have smaller E_g.

Knowledge of electronic structure of polymers is helpful in understanding their electric conduction mechanisms. Polymers with delocalized electronic configuration are capable of being doped to high electrical conductivity.

2.2.3 Band Theory in Conjugated Polymers

The electronic properties of polymers depend on the nature of their bond. The bond formation of macromolecules follows the same principle as that of the diatomic molecules. In any case the bond formation involves the formation of two energy levels, the bonding level and antibonding level. The energy levels before and after bond formation are indicated in Fig. 2.5. For more complex molecules, as each bond is formed, an additional bonding and antibonding level is added to the over all electronic structure [11]. In high-polymer molecules, thousands or millions of atoms may be involved and the number of molecular orbital becomes large. Beyond a certain size of molecule the bonding orbitals crowded together on the energy scale to form a set of closely spaced energy levels. This set is known as a bonding band (valence band). A similar crowding and band formation occurs with the antibonding orbitals, which are described as the conduction band. The two are separated by the energy gap. The band theory for polymer can be helpful in the explanation of the semiconductivity of the polymer. In the next section the electronic properties of the polymer will be presented.

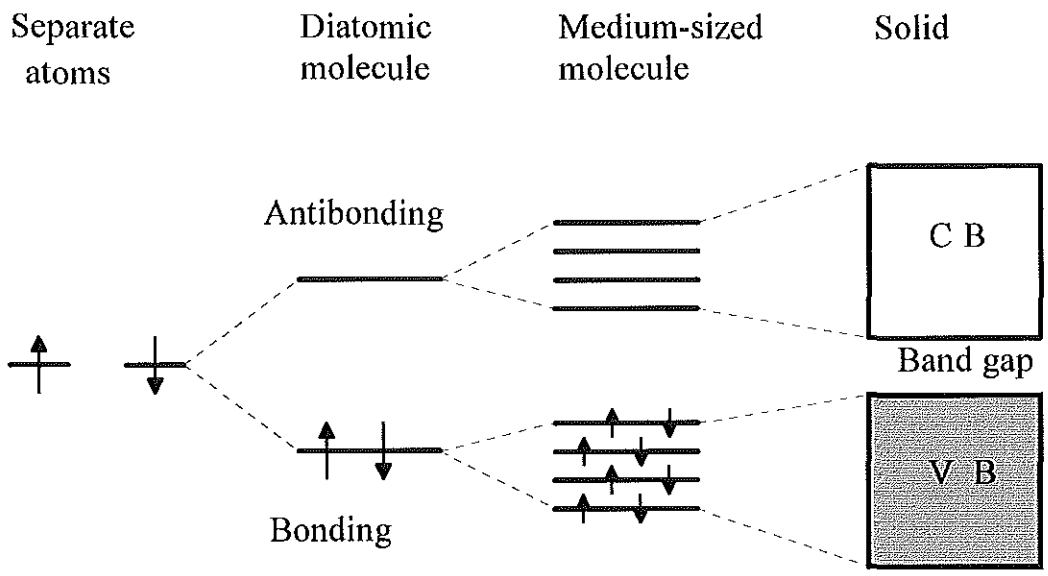

Fig. 2.5 Formation of valence band and conduction band as a result of overcrowding of orbital energy levels into bands.

3 Electronic Properties and Conduction Mechanism in Conjugated Polymers

3.1 Introduction

Polymeric materials have an insulating property and have been used as handles for variety of tools, coating of wires, or for casing of electrical equipment. However, while this is true for most polymers, a special class of these materials called conjugated polymers have electrical and optical properties which are comparable with conventional inorganic semiconductors, metals, or even supper conductors, yet retains the mechanical properties of plastics. Because of the unique features of conjugated polymers in their mechanical and electrical properties they possess, they attract a good deal of fundamental scientific interest. From the practical point of view, these materials also hold great promise for a wide range of applications in electrostatic dissipation, electromagnetic shielding, batteries, electrochromic windows, electronic devices (FET, MISFET, etc.), light emitting diodes (LED) laser, and solar cells [12].

Although the idea of using polymers for their electrically conducting properties dates back to the 1960's, the field really started with the discovery in 1977, when Shirakawa in Japan with his coworkers made polyacetylene conducting. The partial oxidation with iodine or other reagents made polyacetylene films 10^9 times more conductive than they were originally thought. Since then, the dream of combining the processing and mechanical properties of polymers with their electrical and optical properties has driven both the science and technology of conducting polymers [13].

The work in the field of conducting polymers has become highly interdisciplinary with people coming from different areas such as physics, chemistry, material science and engineering all working toward the common goal; controlling the electrical and mechanical

properties of this materials. Early research of conducting polymers focuses on the electrical conductivity of the polymers.

After the discovery of conductivity of polyaceteylene a large number of conducting polymers that include aromatic and heterocyclic polymers and their derivatives have been added. An example of some of these heterocyclic conjugated polymers includes, polythiophene (PT), (and its derivatives), polypyrrole (PPy), polyfuran (PF), poly(paraphenylene) (PPP), polyindole, poly(isothiananphthene), poly(paraphenylenevinylene) (PPV) and some other polymers with heteroatoms in the main chain like polyaniline, PANI. The polymerization process, their chemical structure, morphology and structure and electronic structure and conductivity of these conjugated polymers are discussed in detail in G. P. Evans [14]. Chemical structure and the approximate conductivity of some of these polymers are shown in Fig. 3.1. All conjugated polymers have one thing in common; they contain an extended π-conjugated system, single and double bonds alternating along the polymer chain.

3.2 Doping of Conjugated Polymers

The conductivity of conjugated polymers can be enhanced to higher levels by doping the neutral polymers. Doping is the process of changing the state of oxidation or reduction of conjugated polymers with a concomitant change in the electronic properties of the material. Although the term doping is applied to conjugated polymers, it is different from that of the conventional semiconductors. In semiconductors the dopant species occupy positions within the lattice of the host material, resulting in the presence of either electron-rich or electron deficient sites, with no charge transfer occurring between the two species.

The effect of the dopant boron on silicon for example, arises from the fact that Si has four valence electrons and B has only three, resulting in the creation of electron deficient site

within the lattice i.e., the creation of the positive 'holes'. Similarly, replacing silicon with phosphorus results in electron-rich lattice sites due to the five valence electrons of a phosphorus atom. However, the doping reaction in conjugated polymers is essentially a charge transfer reaction resulting in the partial oxidation or reduction of the polymer, rather than the creation of holes or electrons [14].

In the language of semiconductor physics, the partial oxidation of conjugated polymers is referred to as p-doping and the partial reduction is referred to as n-doping, but the basic process is the removal of electrons in the first case and gain of electrons in the latter case. The doping processes can be represented as shown below.

For p-doping

$$\textbf{Polymer} + \mathbf{X} \rightleftharpoons (\textbf{Polymer})^{y+} + \mathbf{X}^{y-}$$

For n-doping

$$\textbf{Polymer} + \mathbf{M} \rightleftharpoons (\textbf{Polymer})^{y-} + \mathbf{M}^{y+}$$

where **X** is the oxidizing agent and **M** is the reducing agent. $\mathbf{X}^{y-}$ and $\mathbf{M}^{y+}$ are the dopant anion and cation, respectively [15].

Conjugated polymers can be doped either chemically or electrochemically. However, electrochemical doping is emerging as the preferred technique in many applications because it provides a potentially high controllable and reproducible method for investigation of the doping process in which the transfer of charge can be accurately monitored and regulated giving a degree of control which is beyond the scope of gas or solution phase chemical doping [14].

Polymer	Structure	Dopant materials	Approximate conductivity siemens/cm
Polyacetylene		I_2, Br_2, Li, Na, AsF_5	10,000
Polypyrrole	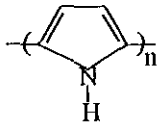	BF_4^-, ClO_4^- tosylate	500 - 7500
Polythiophene	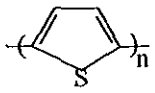	BF_4^-, ClO_4^-, tosylateb $FeCl_4^-$	1000
Poly(3-alkylthiophene)	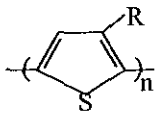	BF_4^-, ClO_4^-, $FeCl_4^-$	1000 - 10000
Polyphenylene sulfide	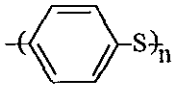	AsF_5	500
Polyphenylenevinylene	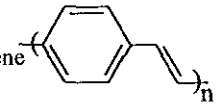	AsF_5	10000
Polythienylenevinylene	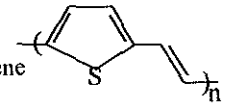	AsF_5	2700
Polyphenylene	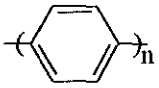	AsF_5, Li, K	1000
Polyisothianaphthene	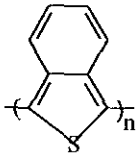	BF_4^-, ClO_4^-	50
Polyazulene	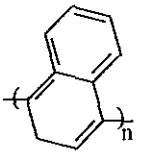	BF_4^-, ClO_4^-	1
Polyfuran	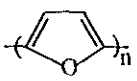	BF_4^-, ClO_4^-	100
Polyaniline	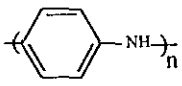	HCl	200

Fig. 3.1 Chemical structure and conductivities of some of conjugated polymers.

3. 3 Electronic Properties

Materials can be classified as metals, semiconductors, or insulators depending on their electrical properties. The electrical properties of any material is determined by its electronic structure. In solid state physics the theory that explains the electronic structure of material is band theory. In insulators and semiconductors we have the highest occupied and lowest unoccupied bands which are called valence band and conduction band, respectively. The difference in energy between conduction band and valence band is called the forbidden energy gap. The electrical properties are controlled by the width of this band gap. For narrow band gap at room temperature thermal excitation of an electron from valence band to the conduction band causes the conductivity. This is what happens in conventional semiconductors. When the band gap is too wide, thermal excitation at room temperature is unable to excite electrons across the band gap and the solid is an insulator. The main difference between semiconductors and insulators lies in the width of the forbidden energy gap. In metals we have partially filled bands, and there is no forbidden energy gap. This is the reason for high conductivity of metals.

However, there are classes of materials known as conjugated polymers which show the electrical properties similar to that of the inorganic semiconductors. Conduction process in them generally depends on the presence of an array of π-conjugated, delocalized double bonds. In the next section their electrical properties will be presented.

3. 3.1 Conjugated Polymers

An electronic structure of some of the conjugated polymers [16] are shown in Fig. 3.1. It is known that there is some relationship between electronic structure of the repeating unit of polymers and its electrical properties. Conjugated polymers contain a property that is common to all of them, an extended π-conjugation, single and double bonds alternating

along the polymer chain. A discussion of various theoretical models (solitons, polarons and bipolarons), to understand the nature of charge carriers for some of the electronic structure of the conjugated polymers are given below, using polyacetylene, and polythiophene as examples.

polyacetylene

The simplest π-conjugated polymer is polyactylene, $(CH)_n$, which is composed of a chain of repeating CH units. It is considered as a prototype conducting polymer. The monomer acetylene is well known as a gas used for welding and it contains unsaturated carbon-carbon bond $(H-C\equiv C-H)$ [17].

The carbon atom has four valence electrons. Three of these electrons form a hybridized sp^2 orbital (i.e. by the overlap of 2s, $2p_x$ $2p_y$ atomic orbitals). The sp^2 orbital has three lobes that are trigonal planar (120^0 apart and in a plane). Two of the lobes form σ-bonds with the two adjacent carbon atoms and the third bonds with the hydrogen atom. The trigonal planar nature of the sp^2 orbitals gives polyacetylene its zigzag backbone structure [12]. The remaining fourth valence electron of each carbon atom occupies the $2p_z$ orbitals that are perpendicular to the plane of sp^2 orbitals. The two $2p_z$ orbitals overlap and form what is known as delocalized π-conjugate system and hence contains one electron per CH group which gives rise to a half-filled electron band.

A half filled π-electron band corresponds to a metallic state of the polymer. Due to the Peierls distortion, however, such a one dimensional metal is unstable with respect to a dimerization of the lattice. And so that the carbon-carbon bonds of the backbone will be distorted by alternating double and single bonds of the linear chain. This dimerization changes the unit cell of the polymer to contain two CH groups, and lowers the total energy of

the system by opening up a band gap (Fig. 3.2), which gives the π-conjugated system semiconducting properties instead of metallic [18].

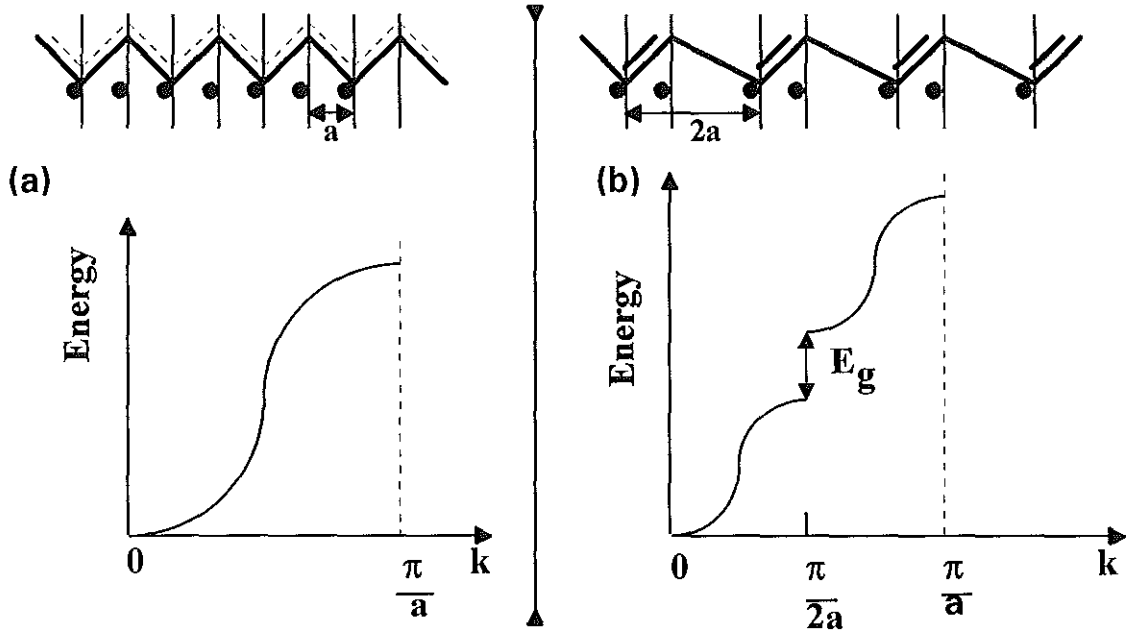

Fig. 3.2 The creation of an energy gap in dispersion relation up on dimerization of polyacetylene. Dispersion relation and density of states for undimerized polyacetylene (a) and for dimerized polyacetylene (b).

A Peierls distortion is a disorder-to-order phase transition in the electronic system and it leads to an energy gap in the dispersion relation (Fig. 3.2) [19]. The dimerization changes the metallic state (Fig. 3.2a) of polyacetylene to a non-metallic state (Fig. 3.2b). In the metallic (undimerized state) all bonds have equal length and the electrons are delocalized over the whole system (dashed line). In non-metallic states (dimerized states) alternating single and double bonds are formed [19].

As a result of an electrostatic interaction between the electrons and the nuclei, the double bonds are shorter than the single bonds. The alternation of bond length is responsible for the

possible structures of the polyacetylene. There are three possible structures of PA. These are trans-transoid, cis-transoid, and trans-cisoid (Fig. 3.3).

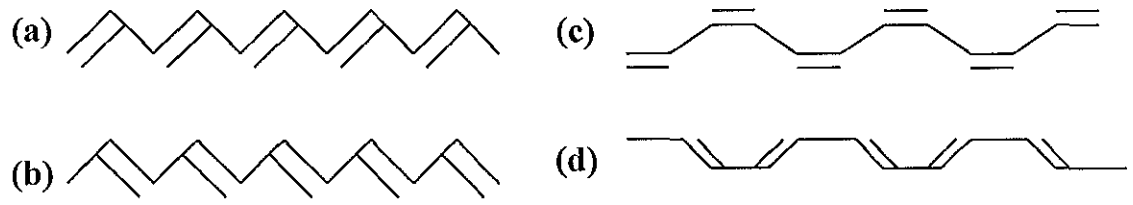

Fig. 3.3 Possible structures for polyactylene chains. Two degenerate trans-structures (a) and (b), and the two non-degenerate cis-structures, (c) cis-transoid and (d) trans-cisoid.

The cis-transoid and trans-cisoid isomers are both of higher energy in contrast to the trans-transoid form and the latter is thermodynamically stable than the other two. The trans-transoid isomer is usually called trans-polyacetylene and it has a property that the single and double bonds can be interchange without any cost of energy, maintaining an equivalent chemical structure. As a result, two energetically degenerate ground state configuration of trans-PA can be formed (Fig. 3.4). Cis-transoid is also simply denoted as cis-polyacetylene. Cis-polyacetylene has a non-degenerate ground state.

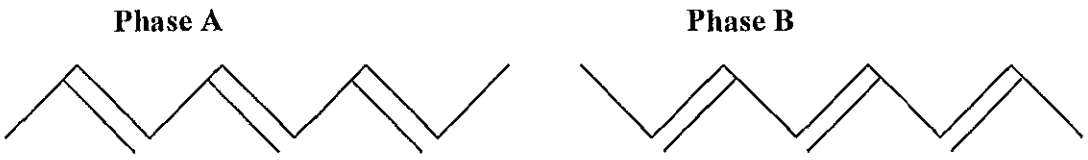

Fig. 3.4 The two degenerate ground state configurations of trans-polyacetylene.

Polythiophene

There are a number of conducting polymers other than polyacetylene, the structure of which are shown in Fig. 3.1. Conjugation is found in several aromatic and heterocyclic polymers. One of which is polythiophene. Polythiophene has a non-degenerate ground state configuration which consists of aromatic thiophene repeating unit. Two bond alternation configurations of Polythiophene are possible, the aromatic and quinoid (Fig. 3.5). The quinoid conformation has higher energy than the aromatic form.

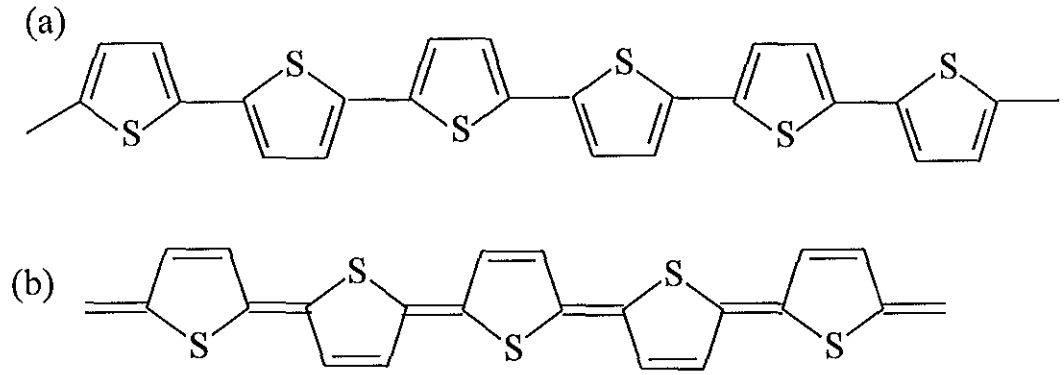

Fig. 3.5 Chemical structure for segments of polythiophene, in the non-degenerate ground state aromatic conformation (a), and in the quinoid conformation (b).

3.3.2 Charge Carriers (Quasi-Particles)

Solitons

As discussed above, PA has two degenerate ground states which is denoted by phase A and phase B (Fig. 3.4). Due to the degeneracy the double and single bonds can be interchanged without changing the ground state energy of the system. If one puts these two chains together a phase transition region will occur, where the two phases have a misfit as shown in Fig. 3.6

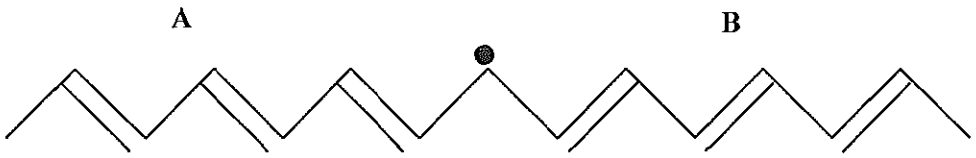

Fig. 3.6 A soliton defect at a phase boundary between the two degenerate trans phases of polyacetylene where the bond alternation has been reversed.

Considering the bonding of carbon atoms on the chain where the defect occurs, the carbon atom between the conjugated segments will be sp^3 hybridized and contains one unpaired electron although the over all charge remain zero. Consequently, a new state (energy level) is created at the mid-gap (i.e. the unpaired electron resides in a non-bonding orbital) (Fig. 3.8) This neutral defect is known as a soliton [14, 17].

A soliton separates a segment of polymer chain with two phases as shown in Fig. 3.6. Hence the soliton in PA is a bond alternation domain wall, a localized region on the chain where the bond alternation reverses. The neutral soliton is singly occupied and therefore has spin ½, and has been calculated to be delocalized over about 15 carbon atoms [14]. Charged solitons can be created upon doping the polymer. Oxidizing or reducing the polymer adds or removes the charges from the polymer chain and this will create a structural defect known as charged solitons and it is located in the mid-gap of the forbidden energy region (Fig. 3.7) [19]. The soliton energy state can contain either zero (positively charged soliton), one (neutral soliton) or two (negatively charged soliton) electrons. Solitons demonstrate the unusual spin charge relation compared to the bare electrons or holes. A neutral soliton (S^0) has spin ½ but no charge, where as a charged soliton ($S^{\pm}$) has no spin.

In conducting polymers, the top of the valence band (the HOMO π-bonding orbital) and the bottom of the conduction band (the LUMO π^*-antibonding) are separated by the forbidden energy region (Fig. 3.7).

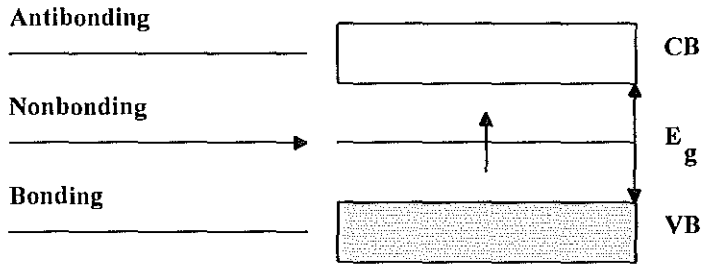

Fig. 3.7 Formation of a mid-gap state. The antibonding (π*) MO and the bonding (π) MO disappear into the conduction band (CB) and the valence band (VB), respectively.

However, when the soliton defect is created it will be located in the mid-gap (where the non-bonding state located) (Fig. 3.7). As can be seen from the band diagram (Fig. 3.8) three possible types of solitons are formed in degenerate ground state conjugated polymers and gives rise to the inherent conductivity of the material.

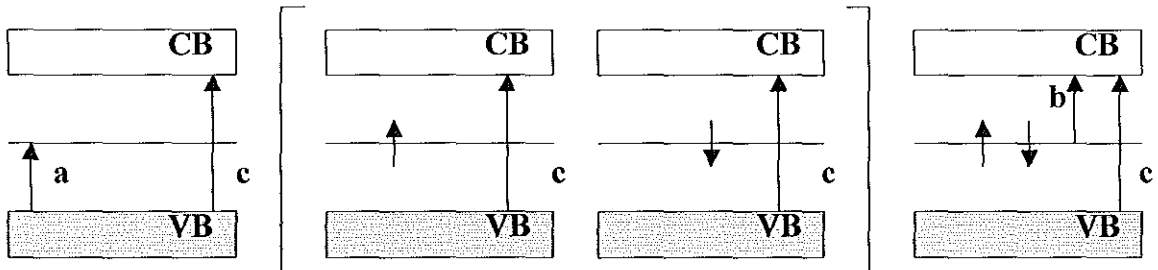

a) Positive soliton, charge +e, spin 0 **b)Neutral soliton, charge 0, spin 1/2** **c) Negative soliton carge -e, spin 0**

Fig. 3.8 Energy level diagram for three possible types of solitons and optical transitions associated with them are indicated with lines a, b, and c.

Polarons and Bipolarons

Trans-polyacetylene is unique in that it possesses degenerate ground state conformation. But all other conjugated polymers including cis-polyacetylene possess non-degenerate states. These will have an important effect on the nature of the charges which they can carry. In polymers with non-degenerate ground state structure, it is also possible to have phase alternation defects up on charge transfer. The phase change will transform the aromatic to a quinoid as shown in Fig. 3.9, using polythiophene.

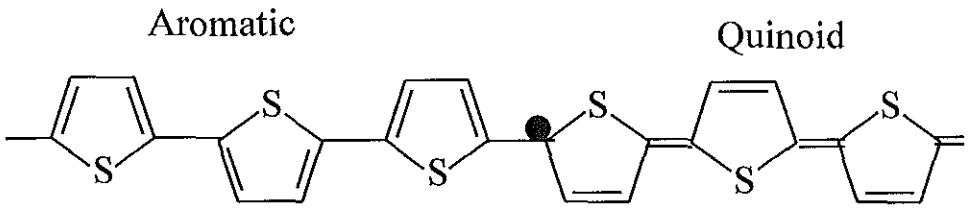

Fig. 3.9 Non-degenerate states of polythiophene where there is transition from the aromatic to the quinoid conformation.

In such polymers, where two regions separated by a topological defect are not degenerate, the formation of single solitons, whether as the result of doping or from inherent defects, is energetically unfavourable and thus the bond alternation must be created in pairs, and a transition back to the aromatic phase will occur somewhere along the chain to have energetically allowed configuration. Unlike trans-polyacetylene where the two bond alternation phases are energetically the same, in polythiophene and in others heterocyclic conjugated polymers, the region of quinoid phase has higher energy than the aromatic phase. In order to minimize the region of higher energy there is attraction between the two alternation defects, and as a result a bound double-defect is created. This confined pair of defects is treated as one defect and is known as a polaron.

In the language of solid state physics the term polaron can be explained as follow. An electron moving in an ionic crystal will polarize its surrounding medium with the result of attracting positive ions and repelling negative ions. The relative motion of the opposite ions gives rise to a polarization field which, in turn, affects the motion of the electron it-self. This electron and its accompanying polarization field is called a polaron [17].

When an extra electron (or hole) is added to a conjugated polymer chain, there is a strongly localized elastic distortion in order to put the charge in a lower electronic energy state. The charge added to the polymer is not a free electron (or hole), but an electron that interacts with a polymer chain by deforming the chain around itself. The resulting defect is called polaron and is defined in standard semiconductor literature as an electron that is dressed by a phonon cloud [12]. Polaron defects can occur in polymers with degenerate as well as non-degenerate ground state configurations.

The formation of bipolarons are similar to that of polarons. But instead of single charge that distorts the lattice as in the case of polarons, there are two electrons (or holes), which are involved in the distortion of the polymer chain. This doubly-charged defect which extends over a similar number of rings (i.e. it is delocalized over about four in PT as in a polaron) is known as a bipolaron.

The bipolarons are formed at high doping levels [20]. On the other hand formation of a polaron can be considered as a combined effect of formation of a neutral and a charged soliton on the same chain. The polaron defect gives rise to the formation of two states in the band gap, symmetrically placed about the mid-gap energy of which one is singly occupied for hole polaron (P^+), and one is doubly and the other is singly occupied for electron polaron (P^-) (Fig. 3.10).

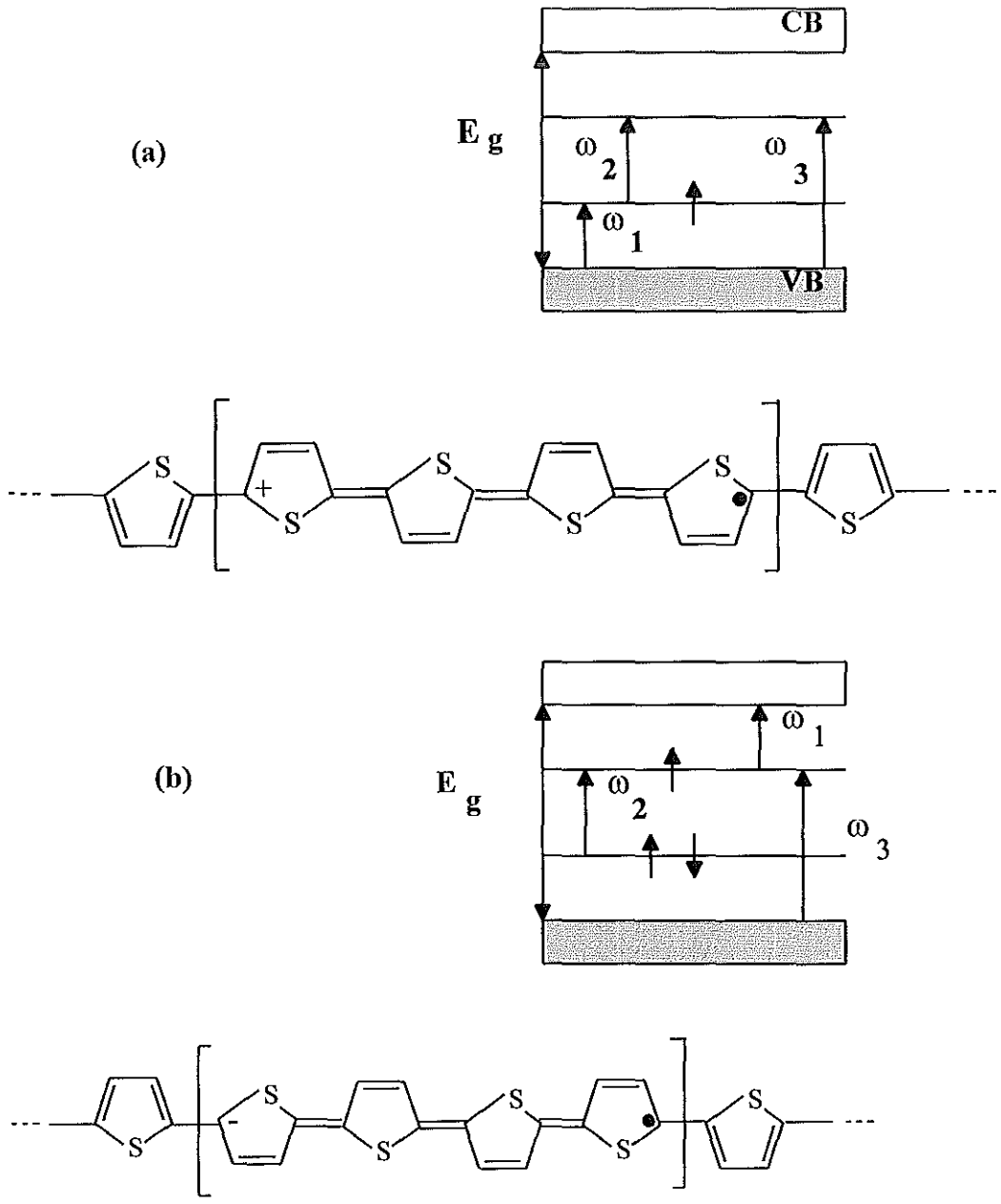

Fig. 3.10 Formation of polaron state in polythiophene.

(a) Hole polaron (P^+), and (b) Electron polaron (P^-).

As stated above when two polarons are introduced to a non-degenerate ground state polymer, a doubly charge bipolaron is formed. Biopolarons have gap states which are either completely filled for negative bipolaron (B^{2-}) or completely empty for positive bipolaron (B^{2+}) as depicted in Fig. 3.11. In contrast to polarons, bipolarons are doubly charge and have

no spin. Bipolaron formation is obtained when the two charges are added to the non-degenerate ground state polymer, and the band diagram and chemical structure of bipolaron is shown in Fig. 3.11.

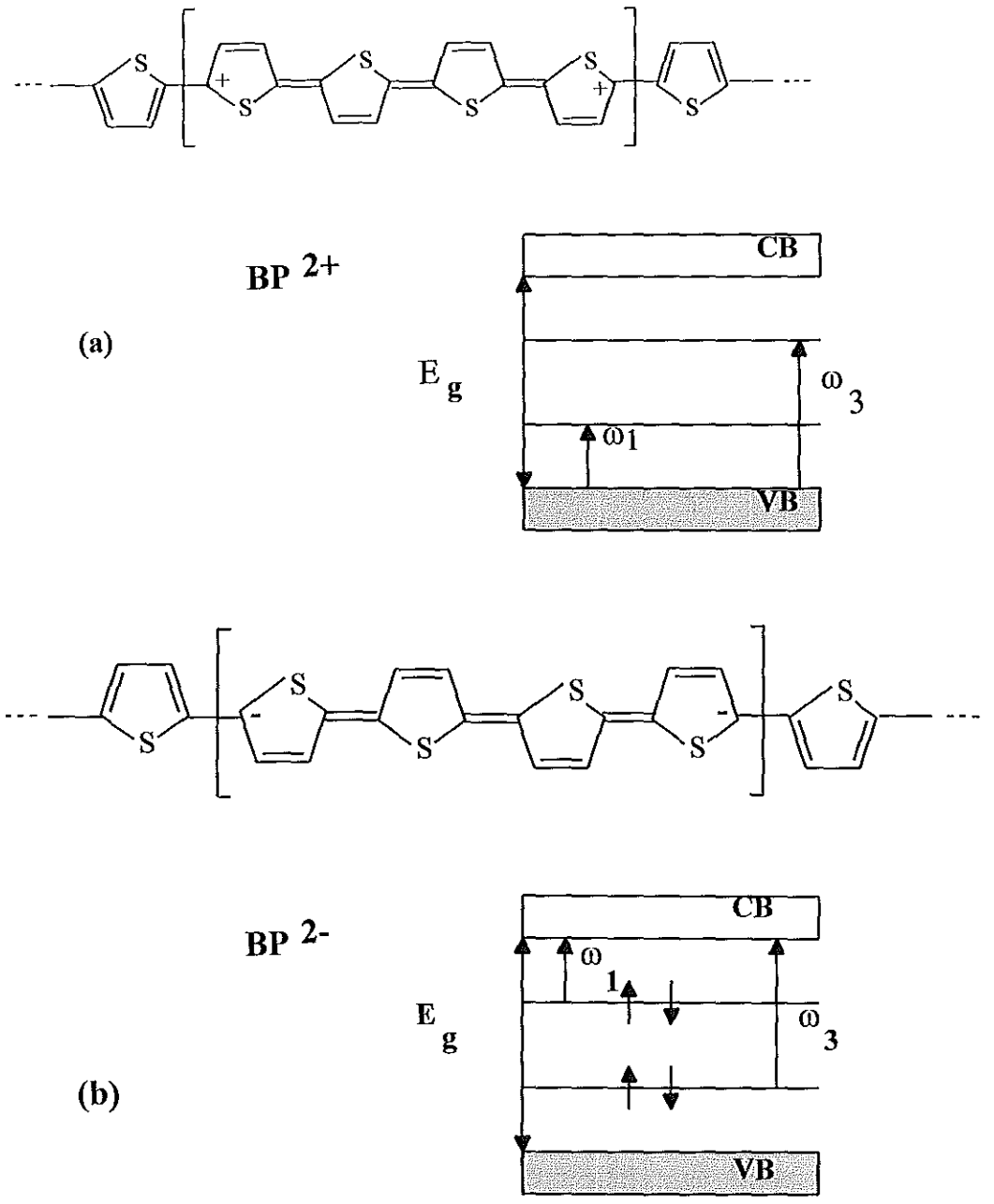

Fig. 3.11 (a) Formation of hole bipolaron in PT, (b) formation of electron bipolaron in PT, and energy level diagrams with possible optical transitions.

Experimental study of optical absorption spectroscopy of conjugated polymers has evidenced the existence of the electronic states in the band gap and supports the polaron and bipolaron picture. For polaron excitation three transitions corresponding to ω_1 , ω_2 , and ω_3 are allowed as is shown in (Fig. 3.10). On the other hand for bipolaron excitations both levels in the gap are either empty or completely filled and carry no spin due to pairing of the electrons. Consequently ω_2 transition is not allowed as is shown in Fig. 3.11. Therefore the absence of spin signal and the ω_2 transition are signatures of bipolarons [20].

Interband transitions from the valence band to the conduction band give each conjugated polymer its specific absorption spectrum. The band gap of neutral conjugated polymers can be determined from the optical absorption spectrum. For example for the neutral PTOPT it was determined [7] to be 2.0 eV.

Optical absorption spectroscopy supported by other experiments confirmed the existence of polarons and bipolarons. It is considered that these charge carriers (quasi-particles) give rise to the conductivity in the non-degenerate ground state polymers. However, it should be born in mind that these models assume ideal structures, and the real polymer system is complex.

3.4 Conductivity

The conductivity of the material is displayed along the wide range of variation. Metals occupy the highest position in the conductivity of the material. The conduction process in metals was explained by a classical Drude model and Sommerfeld theory of metals. Metals are characterized by that they posses unfilled conduction band and partly filled valence band. Hence metals have more energy states available in the valence band than electrons to fill those states, whereas semiconductors and insulators have completely filled valence band and empty conduction band at low temperature and consequently no free charge carriers. Intrinsic

semiconductors and insulators have the same number of electrons as energy states. This is a clear-cut difference between semiconductors and metals.

The conductivity of the metal increases upon decreasing the temperature, while that of the semiconductor increases upon increasing the temperature exponentially. This is because in metals temperature increase enhances the thermal vibrations of the lattice and this increases the scattering of the moving electrons. For semiconductors, temperature increase excites the charge carriers to cross the band gap. On the other hand upon cooling, the charge carriers freeze out and small number of charge carriers are available and conductivity decreases.

A number of theoretical as well as experimental works have shown that the temperature dependence of the conductivity in conjugated polymers resembles that of semiconductors; the conductivity of conjugated polymers decreases with decreasing temperature in general. However there is no single model that could explain the conductivity of polymers. Doping is one important factor that changes the structural and electronic properties of conjugated polymers. For example, the conductivity of polyacetylene can vary by more than 13 orders of magnitude via doping [17]. The complex structural and morphological forms that conductive polymers take, make them difficult to explain their conductivity in one general theory.

Temperature dependence of conductivity is very different in different levels of dopant concentration.

Three different regimes of doping was identified [17] to explain the conductivity of PA. If dopant concentration $y < 0.001$, then the polymer is very lightly doped and in this regime the conductivity is due to hopping. The metallic regime is reached for $y > 0.06$, and the conductivity can be well described by the standard model of extended states. The intermediate region is $0.01 < y < 0.06$. The electrical properties of the intermediately doped samples are typically the most difficult to interpret because there may be several transport

processes, such as thermal fluctuation-induced tunneling, charging energy-limited tunneling and hopping conduction are acting in parallel [21].

Depending on the level of doping we can explain the conductivity of conjugated polymers. Both theoretical calculations and experimental results have shown that the intrinsic electronic properties of a highly doped conjugated polymers are metallic [21]. For highly doped conjugated polymers there is also semiconductive temperature dependence, the model used is that described by Sheng [22, 23]. According to this model small conducting islands with metallic conductivity are separated by resistive barriers. These barriers have been suggested to be conjugational defects, segments of undoped or weakly doped polymer chains, interchain contacts, or other inhomogenties. The charge transport will occur via quantum mechanical tunneling through these barriers. The models of Sheng is the most successful one in describing the conductivity of highly doped conjugated polymers [22].

For small size of highly conducting islands (less than 20 nm) the temperature dependence of the conductivity can be given as [23]:

$$\sigma = \sigma_0 \exp\left[-\left(\frac{T_0}{T}\right)^{\frac{1}{2}}\right] \tag{3.1}$$

where σ_0 and T_0 are material constants.

If the size of the conducting islands are larger (order of a micrometer) the expression for the conductivity is given by [24]:

$$\sigma = \sigma_1 \exp\left(-\frac{T_1}{T_2+T}\right) \tag{3.2}$$

Where T_1 and T_2 are material constants, σ is conductivity and T is absolute temperature.

It is often difficult to distinguish between these two different cases, since the same experimental data can be fitted reasonably well to both when the temperature range is limited.

Lightly doped or undoped conducting polymers show strong temperature dependence of conductivity. The charge transport mechanism is explained by hopping between localized solitonic, polaronic or bipolaronic states according to Mott's Variable Range Hopping theory (VRH) [25, 26]; which was developed to explain the conductivity of amorphous semiconductor.

The term hopping is an abbreviation for the phonon assisted quantum mechanical tunneling of an electron from one localized state to the other localized state. The probability of hopping (ν_{hop}) between two sites at a distance R is given by [17]

$$\nu_{hop} = \nu_{ph} \exp\left\{-2\alpha R - \frac{W \pm eER}{kT}\right\} \tag{3.3}$$

Where the first factor $\exp(-2\alpha R)$ is due to the wave function overlap. It is the probability of finding an electron at a distance R from its initial site, and α is the inverse localization length that describes the exponential decay $\Psi(r) \sim e^{-\alpha r}$ of the electronic wave function at large distances. The second factor, $\exp\left(-\frac{W \pm eER}{kT}\right)$ arises from the electrons need for energy conserving phonon assistance in overcoming the energy difference between sites, where E is external electric field parallel to R, e is charge of an electron, k is Boltzmann constant and W is the energy difference between sites. The plus and minus signs correspond to hopping along and opposite to the electric field direction, respectively.

For weak external electric field, i.e., eER << kT, the probability of hopping is given by

$$\nu_{hop} = \nu_{ph} \exp\left[-2\alpha R - \frac{W}{kT}\right] \tag{3.4}$$

and the hopping conductivity is given by

$$\sigma = 4e^2R^2\nu_{ph}\exp\left[-2\alpha R - \frac{W}{kT}\right] \tag{3.5}$$

Equation (3.5) shows that the hopping conductivity changes with temperature. Depending on the degree of localization we have two types of hopping. If the localization is very strong $\alpha R_0 >> 1$ where R_0 is the nearest neighbour distance, only the nearest neighbour hopping is possible. On the other hand, if $\alpha R_0 = 1$or even less or at very low temperatures, then variable range hopping (VRH) should be expected as first suggested by Mott. There are two competing factors. By increasing the distance the wave function overlap reduces, but the energy difference W is getting smaller and smaller.

The enhanced probability of encountering a smaller W by permitting the electron to choose among the larger selection of final sites contained within a larger neighbourhood, namely a sphere of radius R surrounding the initial site, is expressed by the relationship [25]

$$\left(\frac{4\pi}{3}\right)R^3W(R)N(E_F) = 1 \tag{3.6}$$

where (N_{E_F}) is the density of states at a Fermi-level, and W(R) is the energy for which the number of states spatially located within a sphere of radius R and energetically located within the range from zero to W(R) is, on the average, equal to one. From equation (3.6) W(R) can be written as

$$W(R) = \frac{3}{4\pi R^3 N(E_F)} \tag{3.7}$$

Substituting W(R) for W in equation (3.4) yields

$$\nu_{hop} = \nu_{ph}\exp\left[-AR - B/R^3\right] \tag{3.8}$$

where, $A = 2\alpha$ and $B = \dfrac{3}{4\pi NkT}$.

Minimizing an exponent of equation (3.8) to maximize the ν_{hop} we obtain an expression for the most probable distance as

$$R \approx [\alpha kTN(E_F)]^{-1} \tag{3.9}$$

Substituting equation (3.9) into equation (3.4) and (3.5) we obtain an expression for the maximum hopping rate and the hopping conductivity, respectively as [26]

$$\nu_{hop} = \nu_{ph}\exp\left[-\left(\frac{T_3}{T}\right)^{\frac{1}{4}}\right] \tag{3.10}$$

and

$$\sigma = \sigma_2(T)\exp\left[-\left(\frac{T_3}{T}\right)^{\frac{1}{4}}\right] \tag{3.11}$$

where $T_3 \propto \left(\dfrac{\alpha^3}{kN(E_F)}\right)$ is the characteristic temperature. $\sigma_2(T)$ is more slowly varying than the exponential factor.

The power 1/4 in the term $T^{-1/4}$ enters as the reciprocal of effective dimensionality characteristic of the problem. An electron (a bipolaron in a conducting polymer) can hop to a site which is close to it in four-dimensional space, three space dimension plus one energy dimension, (x,y,z,E). In d dimensions, $\frac{1}{4}$ is replaced by $\frac{1}{d+1}$ and equation (3.11) becomes

$$\sigma = \sigma_2(T)\exp\left[-\left(\frac{T_3}{T}\right)^{\frac{1}{1+d}}\right] \tag{3.12}$$

where d indicates the dimensionality and the corresponding characteristic temperature T_3 now can be expressed as

$$T_3 \propto \frac{\alpha^d}{N(E_F)k} \tag{3.13}$$

The logarithm of the conductivity is proportional to $T^{-1/4}$, $T^{-1/3}$ and $T^{-1/2}$, for three, two and one dimensional conductions, respectively.

The VRH was first developed to describe the charge transport properties in various amorphous semiconductors. But latter works included a number of different modifications inorder to explain conductivity in conjugated polymers as well. For conducting polymers the so called an isotropic VRH-model was developed [21] which takes into account different localization strengths parallel $\left(\alpha_{//}^{-1}\right)$ and perpendicular $\left(\alpha_{\perp}^{-1}\right)$ to the chain direction.

It assumes that the wave function is less localized in the direction of the conjugated chain, so that hops along the chain are favoured. Another difficulty of the VRH theory is that it does not deal with the special types of charge carriers that exist in the conjugated polymers. Kivelson [27] proposed an intersoliton hopping model to explain the interchain charge transfer in conducting polymers. The theory assumes that both charged and neutral solitons coexist in the same sample. Charged solitons are trapped by the dopant counterions, but the neutral are free to move along the polymer chain. when a neutral soliton is close to the charged soliton, the electron hops from one defect to the other, so that interchain transport can occur by hopping between charged and neutral solitons at isoenergetic levels (Fig. 3.12) [19].

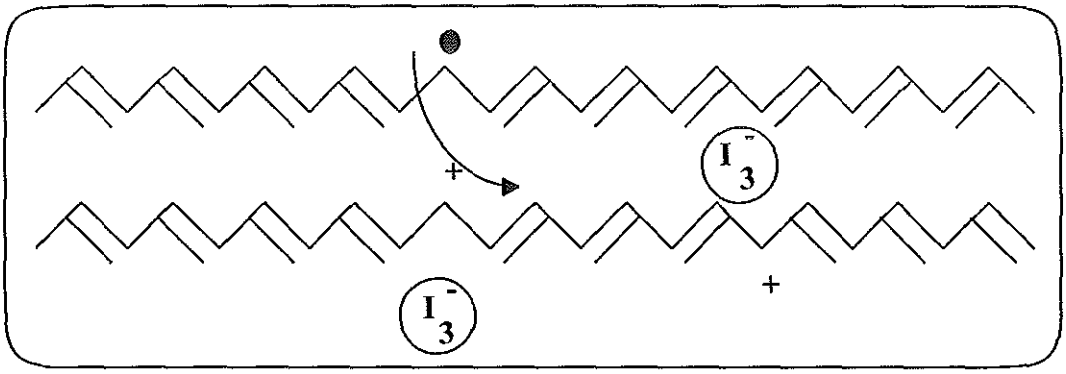

Fig. 3.12 Intersoliton hopping process.

The intersoliton hopping theory was also extended and modified by Kuivalainon et. al., for non-degenerate ground state conjugated polymers as inter polaronic hopping models [28]. A bipolaronic hopping model has also been presented by Chance et. al. [29].

As can be seen from the above description, quite a number of different models exist describing the conduction mechanisms in conjugated polymers. Different models were used to describe the conductivity at different levels of doping. For the moderately doped conjugated polymers interpretation of the conductivity data is even more complex, probably due to a number of different simultaneous charge transport mechanisms. The macroscopic conduction becomes limited by charge transport limitations between fibrils and inhomogeneities in structure and doping levels.

3. 5 Metal-Conducting Polymer Contacts

The metal-semiconductor contact or a Schottky barrier has been known for over a century. The electrical properties of this metal-semiconductor interface has been studied intensively and it has been also used in a wide range of application. Some of the application of

metal-semiconductor contacts are rectifiers, point contact diodes, the gate electrode of field-effect transistors (MESFETs), photodetectors and solar cells.

Apart from inorganic semiconductor-metal contacts, alternative contacts with organic polymers have also been studied. Many reports are available on the Schottky effect of a metal-polymer interface. Therefore, in order to explain the electrical properties of metal-polymer interfaces we use the physics of metal-inorganic semiconductor interface. It is possible to analyze the energy band diagrams of the two basic contacts, a blocking contact or a Schottky barrier in its ideal condition, and an ohmic contact. Blocking or non-ohmic contacts do not allow readily the flow of electrons from the metal to the semiconductor, while the later, ohmic contacts do allow such a flow of electrons.

Both ohmic and rectifying contacts are needed in semiconductor device applications and they have their own importance. When contacts are made between any semiconductor device, or integrated circuit, and the outside world ohmic contacts are needed for minimizing ohmic losses. In the next section the nature of Schottky barriers and its current density-voltage characteristics will be presented. Ohmic contact is also discussed in the subsequent section.

3. 5.1 Schottky Barriers

Schottky barrier diodes are made by depositing a metallic film over a clean semiconductor substrate under very high vacuum conditions (10^{-6} mm of Hg or lower). To understand the properties of the Schottky barrier junction, let's consider the energy band diagram of metal and semiconductor contacts (Fig. 3.13). The energy band diagram for a metal and p-type semiconductor, when they are separated far apart and when they are brought together to form a metal-semiconductor contact are shown in Fig. 3.13a. Similarly for n-type semiconductor the band diagrams are shown in Fig. 3.13b. Before an intimate contact is made we assume that the work functions of the metal (Φ_m) and that of the semiconductor (Φ_{ps}) or (Φ_{ns}) are

not equal. When these two materials with different work functions are brought into contact, the charge carriers will flow from one material to the other until the Fermi levels of both materials are aligned.

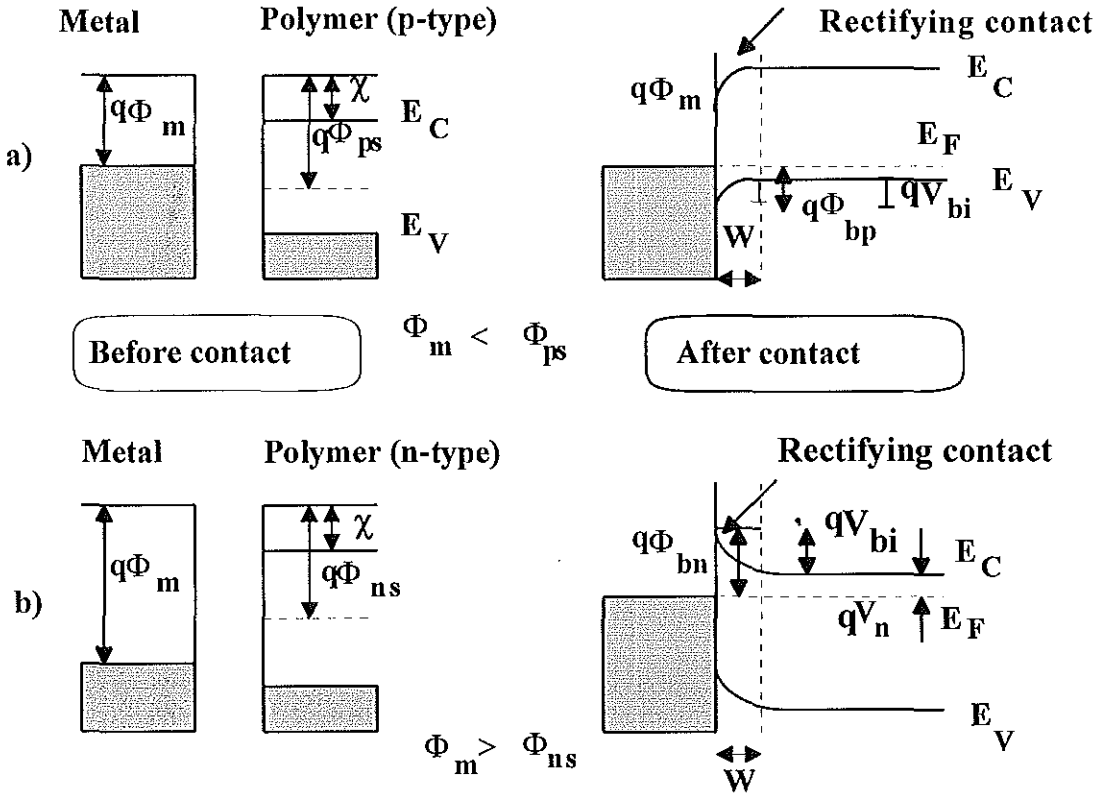

Fig. 3.13 Energy band diagram for Schottky barrier devices.

For high work function metal and n-type semiconductor contact, electrons will flow from semiconductor to the metal in order to equalize the Fermi energies of both materials. Such a net charge carrier flow will set up a positive space charge in the semiconductor and a negative space charge on the metal side of the junction forming layers of charge. The function of this double layer is to set up an electric field to stop any further net flow of the carriers from one material to the other. By similar analysis for contacts between the low work function metal and p-type semiconductor due to the flow of electrons from the metal to

the semiconductor, a negative space charge on the semiconductor and a positive space charge on the metal side will be created.

The work function inequality that determine this two junction behaviors is, $\Phi_m < \Phi_{ps}$ for p-type semiconductor and $\Phi_m > \Phi_{ns}$ for n-type semiconductor. These types of contacts give a blocking or Schottky barrier contacts in the reverse bias voltage. The work function is defined as the energy difference between the energy of vacuum and the Fermi level. It is denoted by $q\Phi_m$ for the metal and $q\Phi_{ns}$ for n-type semiconductor $q\Phi_{ps}$ for the p-type semiconductor. In the ideal Schottky barrier, the height of the barrier for the n-type semiconductor metal junction is given by [30]

$$q\Phi_{bn} = q\Phi_m - q\chi \tag{3.14}$$

Similarly for an ideal contact between a metal and a p-type semiconductor, the barrier height $q\Phi_{bp}$ may similarly be shown to be

$$q\Phi_{bp} = E_g - q(\Phi_m - \chi) \tag{3.15}$$

where χ is electron affinity, the energy separation between the reference vacuum level and the bottom of the conduction band, and E_g the energy difference between the bottom of the conduction band and the top of the valence band $(E_C - E_V) = E_g$. It may be noted that from equation (3.14) and (3.15) that for a given metal-semiconductor contact, the barrier heights on n and p-substrates may be expressed as [30, 31]

$$q(\Phi_{bn} + \Phi_{bp}) = E_g \tag{3.16}$$

The electrons coming from the semiconductor into the metal see a barrier denoted by qV_{bi}, as shown in Fig. 3.13.

The potential barrier qV_{bi} is called the built-in potential and is given by [30]

$$V_{bi} = \Phi_{bn} + V_n \tag{3.17}$$

or

$$V_{bi} = \Phi_m - \Phi_{ns} \tag{3.18}$$

Similarly for the case of p-type semiconductor metal junction where we have $\Phi_m < \Phi_{ps}$, the built-in potential is given by

$$V_{bi} = \Phi_{ps} - \Phi_m \tag{3.19}$$

Current-Voltage Characteristics

The current transport in metal-semiconductor Schottky barrier is mainly due to the majority carriers. A current flow across a Schottky barrier may arise due to any of the following cases: i) Thermionic emission, ii) carrier drift and diffusion and iii) tunneling of the carrier through the barrier. Neglecting the other mechanisms and considering the dominant thermionic emission related current, the current density-voltage characteristics of the Schottky barrier is [30]

$$J_{dark} = J_0\left[\exp\left(\frac{qV}{nkT}\right) - 1\right] \tag{3.18}$$

where J_{dark} is the total current density (dark current density), J_0 is the inverse saturation current density which is the current-density flowing under sufficiently high reverse bias, q is the charge on an electron, V is the applied voltage, n is the ideality factor of the diode (for an ideal diode n = 1), k is the Boltzmann constant, and T is the absolute temperature. The reverse saturation current density J_0 is given by

$$J_0 = A^* T^2 \exp\left(\frac{-q\Phi_b}{kT}\right) \tag{3.19}$$

where A^* is called the effective Richardson constant for thermionic emission. For p-type organic semiconductor Schottky diodes the modified Richardson constant is assumed to be that of a free electron, and is given by $A^* = 120 A/cm^2.K^2$. J_0 is determined by extrapolating the linear part of the plot of lnJ versus V and reading out the intercept. Then the barrier height (Φ_b) can be determined with the help of eqn. 3.19.

The diode ideality factor n can be obtained from the slope of the graph of lnJ vs V. The slope of the plot of lnJ vs V is given by

$$Slope = \frac{\partial \ln J}{\partial V} \tag{3.20}$$

Then the ideality factor n can be deduced easily from the relation given by

$$n = \frac{q}{kT}\left(\frac{\partial \ln J}{\partial V}\right)^{-1} \tag{3.21}$$

Better rectification corresponds to a small value of J_0. On the other hand, when J_0 is very large compared with the current density of experimental interest, the junction will readily pass current for both signs of the applied voltage. From eqn. 3.18 with $J_0 >> J_{dark}$, the exponential term can be expanded to yield,

$$V \approx \left(-\frac{nkT}{qJ_0}\right) J \tag{3.22}$$

Hence for $J_0 >> J$, the contact becomes ohmic.

It is also possible to create metal-semiconductor junctions which have a linear non-rectifying J-V characteristics as given by eqn. 3.22. An ohmic contact between a metal and a semiconductor is defined as one which has a low resistance junction providing current flow

in both directions. There are two possibilities for making ohmic contacts based on work function inequalities [32]. These are: a) to choose metals of low work functions such that $\Phi_m < \Phi_{ns}$ (for metal-n-type semiconductor contacts) for electron injection, or to choose metals of high work functions such that $\Phi_m > \Phi_{ps}$ (for metal-p-type semiconductor contacts) for hole injection, to lower the potential barrier for efficient thermionic emission so as to make the free carrier density higher at the contact than that in the bulk of the semiconductor, and (b) to dope semiconductor surface heavily near the contact to make the potential barrier thin enough for quantum mechanical tunneling. The band diagram for an ohmic contact is different from that of blocking contacts (Fig. 3.13). The energy-band diagram of a metal-n-type polymer and a metal-p-type polymer ohmic contact is shown in Fig. 3.14.

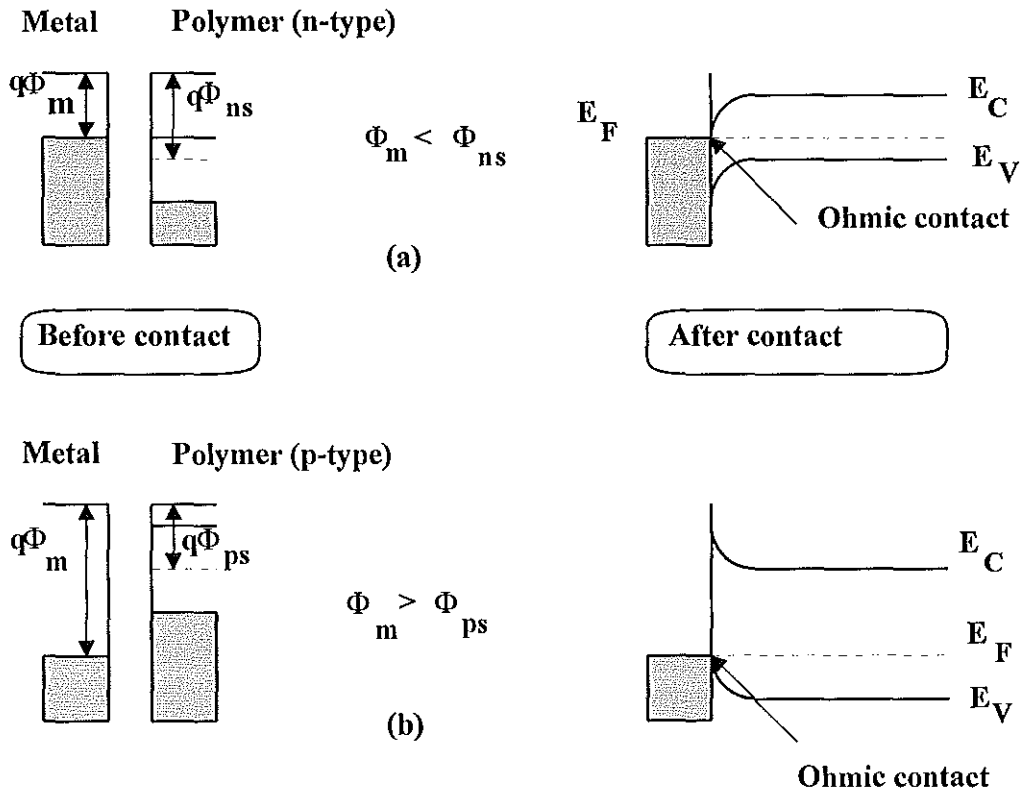

Fig. 3.14 Energy-band diagram before contact and after contact for a metal-n-type polymer junction (a) and for a metal-p-type polymer junction (b) that forms an ohmic contact.

4 PHOTOVOLTAIC ENERGY CONVERSION IN CONDUCTING POLYMERS

4.1 Introduction

In photovoltaic energy conversion, the solar cell converts light energy directly into electrical energy. The materials which are used for this purpose are classified as semiconductors. A tremendous research and development work was made in enhancing efficiency and practical application of solar cells using inorganic semiconductor materials such as silicon, gallium arsenide, sulfide salts of cadmium and copper, and other alloys of these materials . Research work on polycrystalline and amorphous silicon is still active. Moreover, organic semiconductors and conjugated polymers have been also used in devising the solar cells.

The similarity of their electrical and optical properties to the inorganic semiconductors makes the polymers an alternate new material for electronic and optoelectronic devices. Polymeric materials can be considered as n-type and p-type semiconductors. Thus, in the use of these materials for solar cell devices, Schottky barrier theory as developed for inorganic semiconductors can be applied to them. As far as inorganic semiconductor is concerned the most popular junction in electronic industry is the p-n junction, most of the organic diodes are based on an other structure, the metal-semiconductor or Schottky barrier junction. Although it is possible to construct the p-n junction of organic diodes, it is not stable yet. The main source of the instability of a p-n organic diode is the great ability of doping impurities to defuse from the p-to-n side (and vice versa) [33]. Probably this may be one of the reasons why the reports on the photovoltaic effects of conducting polymers mostly uses the metal-semiconductor structures.

It was discussed above that a Schottky barrier is formed at the junction of low work function metals (Al or In) and p-type polymers, while high work function metals (Au, Pt, or ITO) give

ohmic contacts. For an n-type semiconductor the work function inequality to form a barrier or ohmic contact is reverse to that for p-type ones. In the next sections the current-voltage characteristics of the Schottky barrier solar cell in the dark and under illumination will be considered.

4.2 Photovoltaic Effect

The term photovoltaic effect discussed here refers to the development of a voltage across a potential barrier under the influence of light. The electrostatic gradient is created due to the presence of an interfacial region where the net majority carrier density has been depleted from the bulk equilibrium value. Photovoltaic effect in the rectifying Schottky junction can be explained as follows. The absorption of a photon energy greater than the band gap results in the generation of electron-hole pairs or the absorption of a photon creates an exciton rather than free charge carriers [34]. The photovoltaic current in the cell is then a direct transport of the free carriers in the first case while in the second case, in order to generate photocurrents, the excitons must dissociate into electrons and holes either in the bulk of the organic polymer or at metal-polymer interfaces. Hence, in general the sequence that leads to a photovoltiac effect in an organic polymer solar cell device can be described by simple four steps as follows [3, 34]

a. photogeneration of charges

b. charge separation

c. charge transport

d. charge collection to yield current.

4.3 Schottky Barrier Devices

Metal-semiconductor (M-S) is one of the most widely used junction in organic polymer photovoltaic cells. A vast number of reports are available on the photovoltaic effect of such a structure. One of the interests in this type of solar cells is that it is very simple and economical to fabricate, and has a highly improved spectral response at short wavelengths [1].

The structure of Schottky barrier solar cell used in this work is the configuration of glass-ITO/polymer/Al. Generally for p-type materials, the back contact ITO forms a non-blocking (ohmic) contact, while the Schottky barrier formation is realized with Al/p-type conducting polymer contact. ITO exhibits the great advantage of high (>80%) transmittance [35] in the visible region of solar spectrum; thus illumination can be performed from the ITO side. On the other hand Al or In, which forms a rectifying contact, is not transparent to visible light if the films are thick. Thus, the disadvantage is low transmittance of this material layers (e.g. for ~100nm thickness of indium only 1-2% of visible light is transmitted [35]). Insulating thin metaloxide layers may form in the junction interface of these devices.

As mentioned above, the Schottky-type cell formed at Al/PTOPT interface gives photovoltaic properties of the cell. In the next section the solar cell output parameters of the Schottky-type cell will be presented.

4.4 Photovoltaic Parameters

In solar cells the photon energy is converted into electrical energy. When a sheet of solar cell material is exposed to sun light, a photon with energy greater than or equal to the band gap energy, E_g , of the semiconductor is absorbed in the cell thereby generating photocurrent. On the

energy, E_g , of the semiconductor is absorbed in the cell thereby generating photocurrent. On the other hand, a photon energy less than E_g makes no contribution to the cell output. The incident photon energy depends on the wavelength of the light and hence the band gap energy E_g is related to the wavelength. Let's assume, for the sake of simplicity, that the material has a sharp cut off point at a wavelength λ_0 for its absorbance (α) corresponding to its band gap $\left(E_g = \frac{hc}{\lambda_0}\right)$ all the energy of the photons coming from the sun and having longer wavelengths than this cut off point is wasted. All photon energies having shorter wavelengths than this are absorbed [36]. From this basic relation the band gap of the material can be determined. Consequently, the band gap of the polymer PTOPT can be determined from the absorption spectrum.

To derive the solar cell output parameters that are used for characterization of photovoltaic properties of the device, we shall consider an ideal Schottky diode whose band diagram is shown in Fig. 4.1. When the cell is illuminated, the total current density, J, is equal to the sum of the photocurrent density, J_{ph} , and the dark current density, J_{dark} .

$$J = J_{ph} - J_{dark} \tag{4.1}$$

The dark current-voltage characteristics of the Schottky cell can be expressed by eqn. 3.18. Thus the J-V characteristics of the Schottky diodes under illumination is given by

$$J = J_{ph} - J_0\left[\exp\left(\frac{qV}{nkT}\right) - 1\right] \tag{4.2}$$

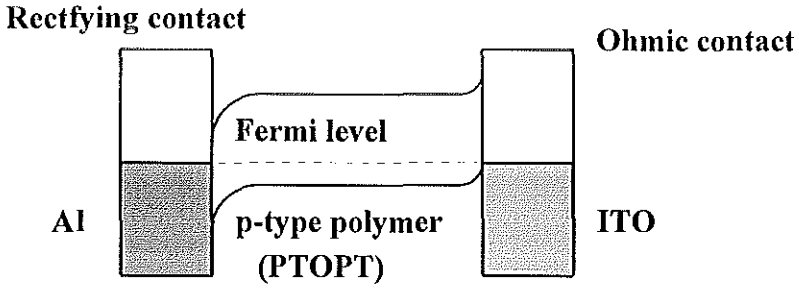

Fig. 4.1 Schematic band diagram for ohmic and rectifying contacts to a p-type polymer.

The ideal J-V characteristics of the solar cells under illumination is shown in Fig. 4.2.

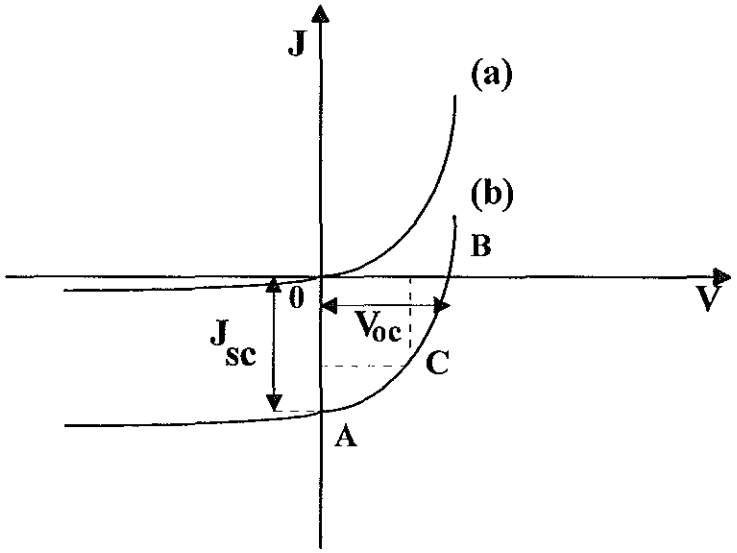

Fig. 4.2 Typical current density-voltage characteristics of Schottky diodes (a) in the dark (b) under illumination.

The three important parameters that are used to characterize the photovoltaic properties of the cell are derived from the J-V characteristics eqn. 4.2 of the Schottky diode.

Short-circuit Current

The short-circuit current corresponds to point A, in Fig. 4.2. It is the condition where photo current flows under zero applied voltage. It is obtained by substituting V = 0 into eqn. 4.2. Ideally it is equal to the current density, J_{ph} , generated by light.

$$J_{sc} = J_{ph} \tag{4.3}$$

Open Circuit Voltage

The open circuit voltage is obtained by setting J = 0 into eqn. 4.2. This is the condition where photovoltage is generated but no photocurrent flows (point B in Fig. 4.2).

$$V_{oc} = \frac{nkT}{q} \ln\left(\frac{J_{ph}}{Jo} + 1\right) \tag{4.4}$$

Fill-factor (FF)

An other important parameter of solar cell is the fill-factor, FF, defined as

$$FF = \frac{V_{mp}J_{mp}}{V_{oc}J_{sc}} \tag{4.5}$$

where V_{mp}, J_{mp} are the voltage and the current at the maximum power point (point C Fig. 4.2). It measures the squarness of the J-V characteristics. Ideally it is the function of V_{oc} , and is given by an empirical expression as follows [37]:

$$FF = \frac{v_{oc} - \ln(v_{oc} + 0.72)}{v_{oc} + 1} \tag{4.6}$$

Where $v_{oc} = V_{oc} / \left(\frac{kT}{q}\right)$ is the normalized voltage.

Efficiency

The energy conversion efficiency of the solar cell in converting light energy into useful electrical energy is the most important quantity defining the quality of the cell. In the J-V curve of the Schottky diode (Fig. 4.2) point C corresponds to the maximum power point, where the product of photovoltage V_{mp}, and photocurrent, J_{mp}, is maximum. The energy conversion efficiency, η, is then given by

$$\eta = \frac{V_{mp}J_{mp}}{P_{in}} = \frac{V_{oc}J_{sc}.FF}{P_{in}} \tag{4.7}$$

where P_{in} is the intensity of the light incident on the cell.

5 EXPERIMENTAL DETAILS

In this section the apparatus and experimental set ups that are used for sample preparation and measurements of electrical and photovoltaic properties of the device are described. A short instrumental description is given.

5.1 Experimental Apparatus

5.1.1 Spinner System

The spinner system (model 4000) is used for spin coating of the polymer solution on a glass substrate to prepare a uniform thin film. It provides an economical and simple method for thin film preparation.

The general features of this apparatus are :

1. It is suitable for coating up to 5" diameter wafers/substrate (polymers/substrate).
2. It consists of electronically controlled spin speeds from 100rpm to 6200rpm.
3. There are three fully automatic sequenced spin operations.
4. A remote control unit controls all functions.

5.1.2 AUTO 306 Vacuum Depositor

The AUTO 306 vacuum depositor is used for variety of coatings under a high vacuum condition. It was designed for physical vapor deposition process. It is used for evaporation of metals like Al, Au, Pt, and In to deposit on the polymer-on-glass substrate that can be the desired metal contact to the polymer. The deposition process is made under high vacuum condition at a very low pressure (~10^{-7} Torr). It is used for the deposition of aluminum on the PTOPT/glass substrate at a pressure of approximately 10^{-6} Torr.

5.1.3 Perkin Elmer λ19 UV/VIS/NIR Spectrophotometer

The absorption spectrum of PTOPT (undoped) was recorded by using a Perkin Elmer λ19 UV/VIS/NIR spectrophotometer. It has a double beam, double monochromator, and measures a ratio of two beams operating in the ultraviolet, visible and near infrared (NIR) spectral ranges. The instrument is controlled via an external personal computer using, the UV computerized spectroscopy software. The operating procedures are according to the instruction in the manual of Perkin Elmer.

5.1.4 HP Model 4140B pA Meter/Dc Voltage Source

The current-voltage characteristics was measured by using the HP model 4140B pA meter. It comprises a highly stable pA meter with 10^{-15} A (max.) resolution coupled with two programmable DC voltage sources to ensure useability in different applications. It has an ability to make accurate I-V measurement. It can automatically synchronize measurement timing between the pA meter section and the voltage source section when the function is set to I-V. The I-V measurement was made with a stair case waves. The start, stop and step voltage can be set from -100V to +100V at 100mV resolution and from -10V to +10V at 10mV resolution. The later situation is used for the I-V measurement made in this work.

5.1.5 Optical Bench

Figure 5.1 shows a schematic description of the optical bench and apparatus associated with it. Power supply, lamp housing, sample holder and the out put measuring instrument (HP pA meter) are indicated. This experimental set-up is the main arrangement that is used in the photovoltaic characteristics measurement of the device. The power supply is used to illuminate

the sample. The data collected by the use of HP pA meter was analyzed by a personal computer. The intensity of the light incident on the sample was measured by a Lux meter at the sample position.

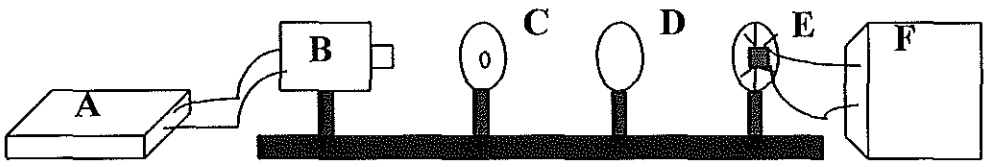

Fig. 5.1 Experimental set-up for the photovoltaic measurement. (A) power supply, (B) lamp housing, (C) shutter, (D) lens, (E) sample holder, and (F) an output measuring instrument (HP pA meter).

5.2 Sample Preparation

In this section a description of sample preparation is presented. Two types of samples are prepared one is thin film of the conducting polymer PTOPT on the glass substrate which was used for band gap determination and the second one is the photovoltaic cell whose configuration is Al/PTOPT/ITO-glass structure and it was used to characterize the photovoltaic properties of the conjugated polymer.

A solution of undoped PTOPT in chloroform (5mg/ml) is dropped on a clean glass substrate and it is spin coated by using spinner system. The spin rates of the spinner determines the thickness of the samples prepared. Various spin rates are used in order to get samples of different thickness for investigation. The samples thus prepared has PTOPT/glass structure and they are

only used to perform the absorption spectrum measurement to determine the band gap of PTOPT.

Although the sample used for the J-V measurement was not prepared here, description of preparation of the sample is made for the sake of completeness. The device Al/PTOPT/ITO, can be prepared as it was previously reported [7] and it was explained as follows. Indium-Tin-Oxide (ITO) coated glass is prepared and this is cut into the desired size of the cell. Part of the ITO is then covered by photoresist and the exposed ITO is etched out of the glass with a mixture of concentrated HCl, HNO_3 and water 48: 4: 48 by volume. The purpose of etching part of the ITO from the glass is to provide a region suitable for electrical contacts to the aluminum layer deposited later. The photoresist is removed by using aceton, and the surface is washed successively with detergent (Decon), distilled water and ethanol.

A polymer PTOPT dissolved in chloroform (5mg/ml) is then spin coated on the ITO/glass substrate by means of spinner system and thin film of PTOPT/ITO-glass is produced. The thickness of the film thus prepared is measured by DEKTAK 3030 surface profilometer and it was found to be 200-300nm. Finally to get a complete structure of the diode, 120nm thick aluminum strips are vacuum evaporated at a pressure of $\sim 3 \times 10^{-6}$ Torr using a vacuum depositor. Deposition of aluminum is such that part of the strip is on the PTOPT/ITO, while the remaining part is over the bare glass from which the ITO is etched out. This is to avoid the possible damage of Al and the polymer beneath when attaching electrical contacts. Now we have a complete metal contacts to the polymer, Al as a schottky contact and the ITO as an ohmic contact [19]. The device thus prepared has an Al/PTOPT/ITO-glass sandwich structure. The effective area of the device was $0.06cm^2$. This device is then used for current density-voltage measurement in the dark and under illumination. The configuration of the Schottky cell and the

chemical structure of the polymer PTOPT are shown in Fig. 5.2.

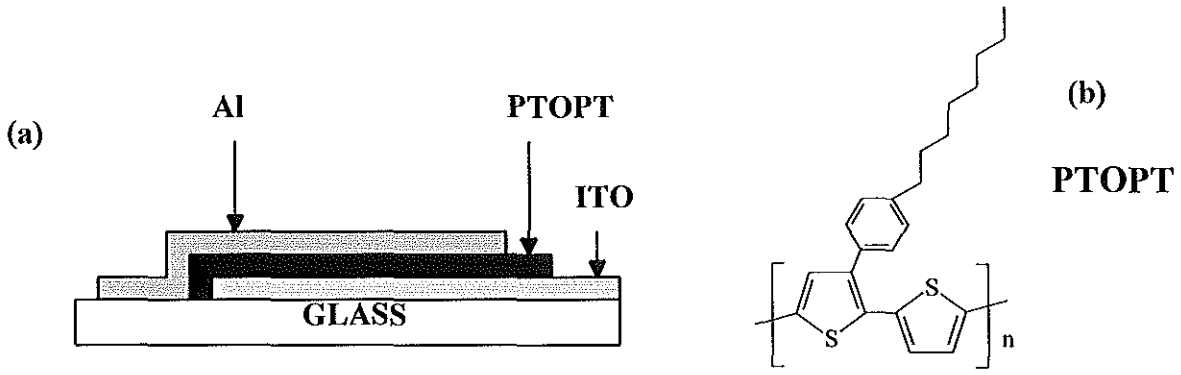

Fig. 5.2 (a) Al/PTOPT/ITO-glass sandwich structure, and (b) chemical structure of PTOPT.

5.3 Current Density-Voltage Measurements

The current density-voltage (J-V) characteristics in the dark, as well as under illumination was measured by means of HP pA meter (model 4140B). A linear sweep voltage applied was from -3V to +3V. The voltage is increased at 0.1V intervals with hold time and step delay time of 1second. The data collected is then analyzed using personal computer.

For photovoltaic measurements the sample was illuminated through ITO side by a tungsten halogen lamp with a stabilized power supply. The cell was illuminated by a white light, whose intensity was measured at the position of the sample with an electronic Luxmeter (model Lux-101). The intensity of the light incident on the cell was approximately 100mW/cm^2. The same procedures are used for the J-V measurements in the dark and under illumination. All the measurements were carried out at the ambient temperature and the experiment was performed about three months after the date of preparation of the sample.

6 RESULTS AND DISCUSSION

6.1 Absorption Spectrum

Figure 6.1 shows the absorption spectrum of PTOPT. The semiconductive behavior of PTOPT was confirmed by measuring the absorption spectrum of PTOPT/glass substrate by Perkin Elmer λ19 UV/VIS/NIR spectrophotometer. Background correction was made before taking the data of absorption spectrum. From the spectrum of absorbance versus energy the band gap energy of PTOPT can be deduced. The threshold energy of the absorption is assumed to correspond to the band gap energy through the relation $E_g = \frac{hc}{\lambda}$. The band gap energy determined from the absorption spectrum is 2.0eV. This result is consistent with previously reported observations [7].

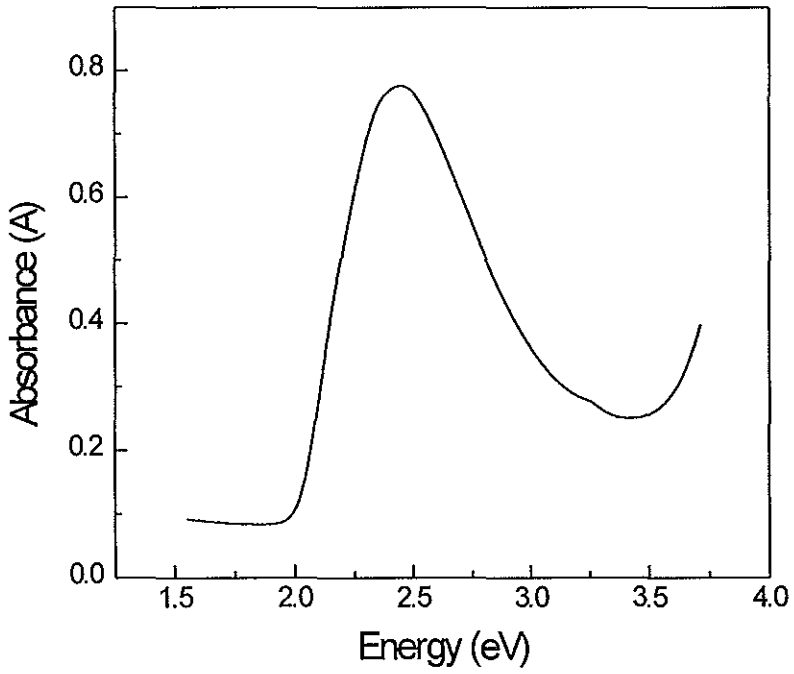

Fig. 6.1 Absorption spectrum of undoped PTOPT.

6.2 Current Density-Voltage (J-V) Characteristics

6.2.1 Dark J-V Characteristics

The current density-voltage characteristics of Al/PTOPT/ITO Schottky diode in the dark is shown in Fig. 6.2. The device exhibits a rectification character in the dark. The rectification ratio of 2.2×10^3 is obtained at $\pm 3V$. The rectifying character in Al/PTOPT/ITO device indicates that Schottky junction is formed at the Al/PTOPT interface. Since PTOPT is considered as a p-type semiconductor, the rectification effect can be explained by the small work function metal, Al, and p-type semiconductivity of the polymer which forms the Schottky barrier at Al/PTOPT interface, where the conduction band and the valence band bend downwards at equilibrium (Fig. 4.1). On the other hand the PTOPT/ITO interface forms an ohmic contact because the work function of ITO is greater than that of PTOPT. This was confirmed using PPy/Au [38].

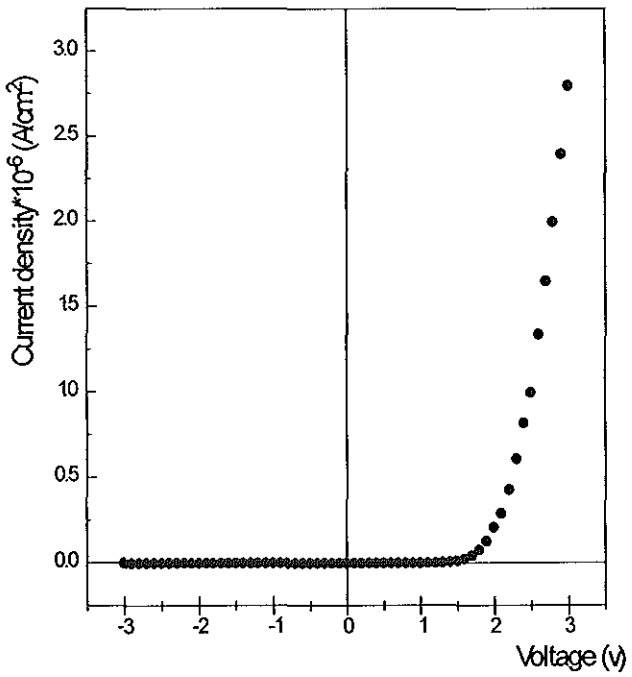

Fig. 6.2 Dark current density-voltage characteristics of neutral PTOPT.

From the J-V curve it can be seen that the forward current increases exponentially at a lower forward voltage region and increases linearly at the higher forward voltage region. Forward current is defined here as that corresponding to the application of a negative voltage to the aluminum.

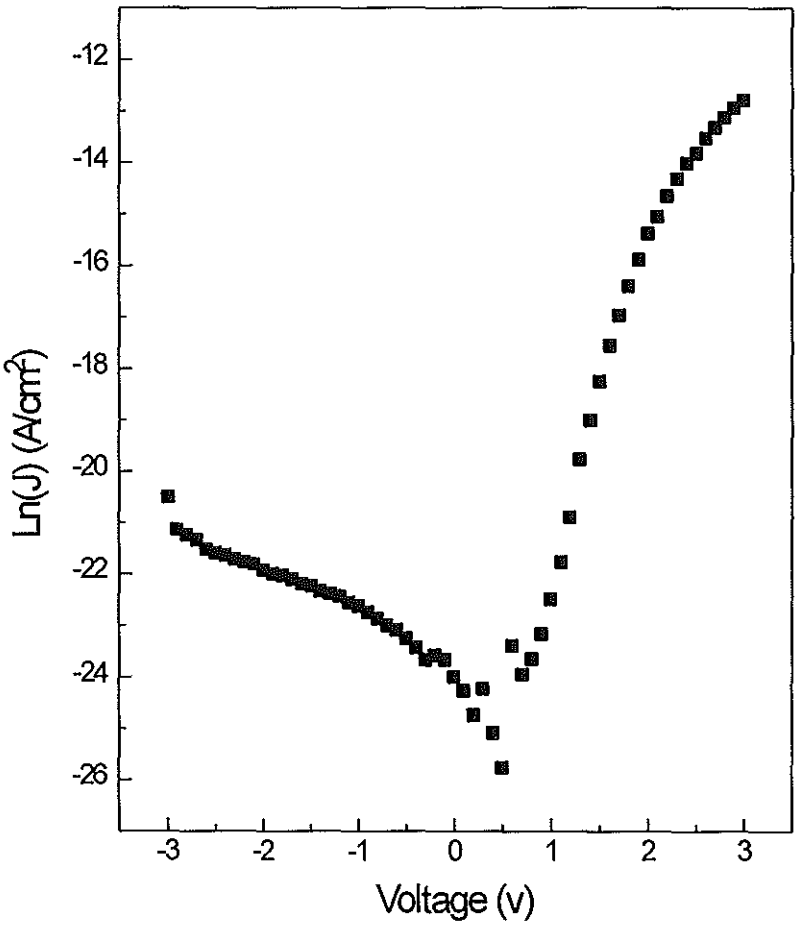

Fig. 6.3 Semi-log plot of J-V for neutral PTOPT.

A semi-logarithm plot (Fig. 6.3) of the current density versus voltage of the same diode also shows that the forward current increases exponentially in the applied voltage between 1.0V and 2.0V. This exponential dependence in the lower forward voltage region can be attributed to a

formation of depletion region near the Al/PTOPT interface (Fig. 4.1). From Fig. 6.3 it can be also observed that the current density deviates from its exponential dependence on the voltage at high forward voltage (> 2.0V). This behavior may be attributed to that the current at high voltages is limited mainly by ohmic losses in the bulk resistance of the PTOPT.

In Schottky barrier diodes, the J-V characteristics obey the well known Shockley equation and the dark current density is given by eqn. 3.18. The expression for J_0 depends on how the charge transport is modeled. For the Schottky barrier devices the charge transport is usually assumed to be due to thermionic emission of the charge carriers over the potential barrier. Thermionic emission theory can be applied to our device and hence the current is assumed to be controlled only by the transfer of carriers across the Schottky (Al/PTOPT) interface. Therefore, J_0 is due to the thermionic emission of the majority charge carriers across the potential barrier, and it is given by Richardson equation as it was expressed in eqn. 3.19.

For the voltage range between 1.0V and 2.0V the experimental data plotted as lnJ vs V (Fig. 6.3) gives almost a linear curve; thus the term -1 in eqn. 3.19 can be neglected as $qV/nkT >> 1$. The intercept of lnJ vs V on the vertical axis extrapolated backward will give the saturation current density J_0 and it was obtained to be $6.7 \times 10^{-14} A/cm^2$. The barrier height Φ_b can be calculated from the value of J_0 obtained and it is found to be about 1.2V. Compared to an earlier results [7] the values of J_0 and the barrier height Φ_b obtained in this study agree to a certain extent.

The ideality factor n of the diode was obtained from the slope of the plot of lnJ vs V through the relation given by eqn. 3.21. The value of the ideality factor is thus n = 4.0 and this high value of the ideality factor can be attributed to the recombination of electrons and holes in the depletion region. The junction parameters obtained from the J-V measurements are summarized in table 6.1.

Table 6.1 Electrical parameters obtained from J-V measurements of the Schottky diode made from neutral PTOPT

Parameters	Values	Units
J_0	6.7×10^{-14}	A/cm^2
Φ_b	1.2	V (volts)
E_g	2.0	eV
γ	2.2×10^3	
n	4.0	

6.2.2 Photocurrent Density-Voltage (J-V) Characteristics

The rectifying property of the device in the dark indicates that PTOPT/Al has desirable photovoltaic property. Photovoltaic properties of the device is investigated and the results obtained are presented below.

Figure 4.1 shows the qualitative energy band diagram that may be formed at the Al/PTOPT/ITO junction. The effect of light on the Schottky barrier cell produces an electron-hole pair by each absorbed photon. If the generation occurs via an excitonic mechanism, the exciton can then diffuse through the bulk of the polymer towards the interface, and subsequent dissociations of the excitons take place, resulting in free charge carriers. Generally, photocurrent generation involves the process of light absorption, photogeneration of charge carriers, diffusion of charge carriers and finally collection of charges to produce current. Since PTOPT is considered as a p-type semiconductor, holes or hole polarons are the dominant charge carriers and contribute to

the photocurrent measured in our device. The generated hole polarons under illumination of light move towards the metal Al, while the electrons go to the PTOPT/ITO junction.

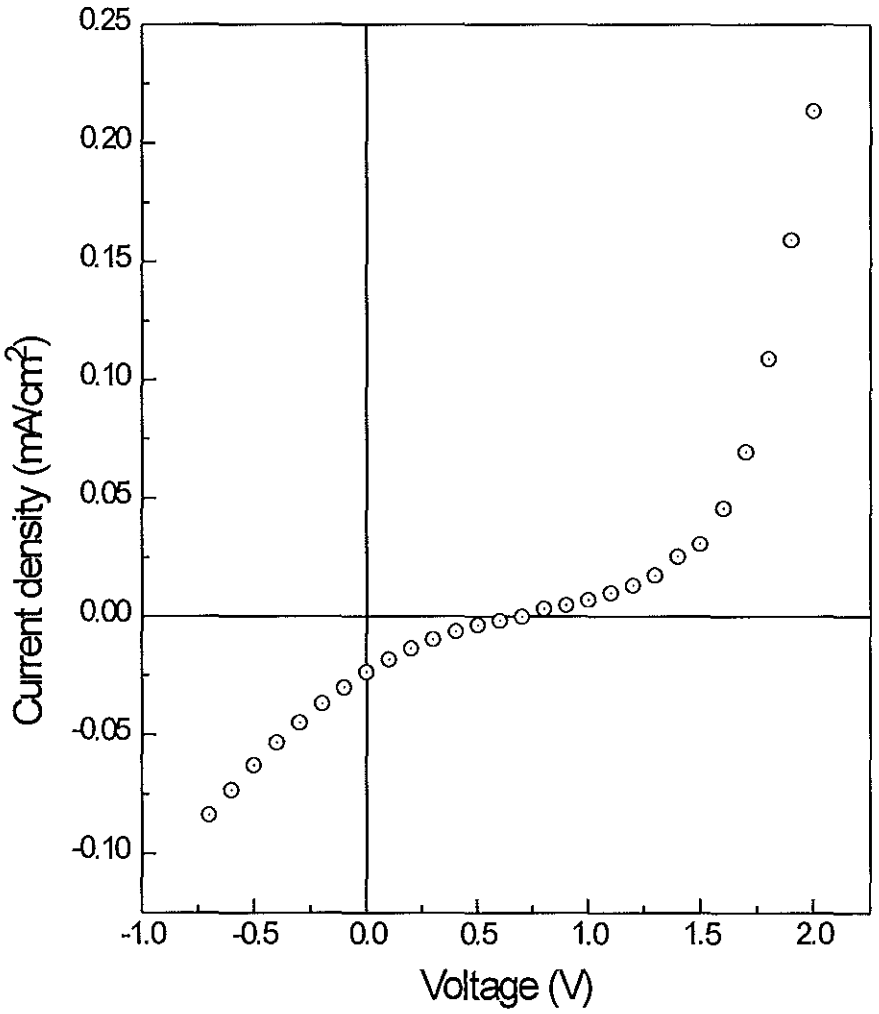

Fig. 6.4 Photocurrent density-voltage characteristics of Al/PTOPT/ITO device.

The photocurrent density-voltage characteristics of the device is depicted in Fig. 6.4. The typical photovoltaic parameters have been calculated from the analysis of J-V characteristics and listed in table 6.2. The illumination was made by white light from halogen source. The intensity of the

light measured at the sample position is approximately 100mW/cm^2. The effective area of the solar cell was 0.06cm^2. The short-circuit current density and the open-circuit voltage of the device are $J_{sc} = 2.5 \times 10^{-5} A/cm^2$ and V_{oc} = 0.75V respectively. The fill-factor defined as the ratio of the maximum power to the product of the open-circuit voltage and short-circuit current is obtained as, FF = 0.2. The power conversion efficiency η = 0.004% is obtained. The efficiency obtained is low as it is generally the case for other types of organic solar cells. However, the main cause of these low values is the old age of the sample since they were characterized three months after they were prepared.

Table 6.2 Photovoltaic parameters of Al/PTOPT/ITO device.

Parameters	Values	Units
J_{sc}	2.5×10^{-5}	A/cm^2
V_{oc}	0.75	V (volts)
FF	0.2	
η	0.004	%

7 CONCLUSION

The electrical and photovoltaic properties of the Schottky junction having a configuration of Al/PTOPT/ITO-glass have been studied. The results obtained are explained from the point of view of Schottky barrier theory applied to the Al/PTOPT interface. Conjugated polymer PTOPT is a p-type semiconductor. The absorption spectrum of PTOPT reveals that the polymer has a band gap of 2.0eV. The rectification ratio observed at $\pm 3V$ is about 2.2×10^3. This indicates that the barrier is formed at the Al/PTOPT interface. The high ideality factor (n = 4.0) obtained indicates that there are defects which leads to the high probability of electron-hole recombination in the depletion layer. From photovoltaic measurements it has been shown that the Al/PTOPT/ITO has a photovoltaic property converting light energy into electrical energy. The effective area of this device was 0.06cm^2. The open-circuit voltage and the short-circuit current density for the cell are 0.75V and $2.5 \times 10^{-5} A/cm^2$, respectively, under illumination of white light whose intensity is ~100mW/cm^2. The fill-factor and the photovoltaic energy conversion efficiency obtained are 0.2 and 0.004% respectively. It can be concluded that the device Al/PTOPT/ITO shows photovoltaic properties, and further studies on its photovoltaic properties can be made in order to investigate the device performance improvement and to obtain better experimental results from freshly prepared samples. Spectral response is another aspect that should be further investigated.

8 REFERENCES

1. H. J. Hovel, *Semiconductors and Semimetals*, Vol. II, Solar Cells, academic press, New York, 1975.
2. D. M. Champin, C. S. Fuller, and G. L. Pearson, *J. Appl. Phys.*, 25 (1954) 676.
3. D. A. Seanor, *Electrical Properties of Polymers,* academic press, New York, 1982.
4. W. Bantikassegn and O. Inganas, *J. Phys. D: Appl. Phys.*, 29 (1996) 2971.
5. Show-An Chen and Y. Fang, *Synthetic Metals*, 60 (1993) 215.
6. W. Bantikassegn and O. Inganas, *Thin Solid Films,* 293 (1997) 138.
7. W. Bantikassegn and O. Inganas, Synthetic Metals, 87 (1997) 5.
8. Y. Greenwald, J. Poplawski, E. Ehren Freud and S. Speiser, *Synthetic Metals,* 85 (1997) 1353.
9. M. Smith, *Organic Chemistry,* Harper Perennial, 1993.
10. J. Mc Murry, *Organic Chemistry*, Brooks, Monterey, 1984.
11. H. R. Allcock, and F. W. Lampe, *Contemporary Polymer Chemistry, 2nd edn.,* Prentice-Hall, New Jersy 1990.
12. L. B. Smilowitz, *Circuits and Devices Magazine,* Jan. 1994: 19-23.
13. W. R. Saleneck and J. L. Bredas, *Solid State Communications,* Vol. 92, Nos. 1-2, pp. 31-36, 1994.
14. G. P. Evans, *Advances in Electrochemical science and Engineering,* Vol. 1, VCH Verlagsgesell Schaft mbH, 1990.
15. Y. Teketel, *All-Soid-State Photoelectrochemical Solar Energy Conversion,* Ph.D. dissertations, Addis Ababa, 1997.
16. M. G. Kanatzidis, *Conductive Polymers, Special Reports,* Dec. 3, 1990.

17. Yu Lu, *Solitons and Polarons in Conducting Polymers,* World Scientific Publishing Co Pte Ltd., 1988.

18. F. Claes, *Theoretical Studies of Metal/Conjugated polymer Interactions,* Ph.D. dissertations, Linkoping, 1993.

19. W. Bantikassegn, *Electronic Properties of Junctions Between Aluminium and Doped Polyheterocycles,* Ph.D. dissertations, ISBN, Linkoping, Sweden, 1996.

20. G. Harbeke, D. Baeriswyl, H. Kiess and W. Kobel, *Physica Scripta,* Vol. T13, (1986) 302.

21. H. Stubb, E. Punkka and J. Paloheimo, *Materials sciences and Engineering,* 10 (1993) 85.

22. P. Sheng, Phys. Rev. B, 21 (1980) 2180.

23. P. Sheng and J. Klafter, *Phys. Rev.* B, 27 (1983) 2583.

24. P. Sheng, E. K. Sichel and J. I. Gittleman, *Phys. Rev. Lett.* , 40 (1978) 1197.

25. R. Zallen, *The physics of Amorphous Solids,* John Wiley & Sons, New York, 1983.

26. N. F. *Mott, Phil. Mag.* 19 (1969) 835.

27. S. Kivelson, *Phys. Rev.* B, 25 (1982) 3798.

28. P. Kuivalainen, H. Stubb, H. Isotalo, P. Yil-Lathti and C. Holmstrom, *Phys. Rev.* B, 31 (1975) 7900.

29. R. R. Chance, J. L. Berdas and R. Silbey, *Phys. Rev.* B, 29 (1984) 4491.

30. S. M. Sze, *Physics of Semiconductor Devices,* John Wiley & Sons, 2nd edn. , New York, 1981.

31. D. K. Roy, *Quantum Mechanical Tunneling and its Applications,* World Scientific, Singapore, 1986.

32. K. C. Kao, and W. Hwang, *Electrical transports in Solids, With practical reference to Organic Semiconductors,* Oxford, 1981.

33. G. Horowitz, *Adv. Mater.* 2 (1990) No. 617.

34. A. K. Ghosh and T. Feng, *J. Appl. Phys.* , 49 (12): (1978) 5982.

35. D. Wohrle and D. Meissner, *Adv. Mater.*, 3 (1991) No. 3.

36. H. Tsubomura and H. Kobayashi, *Critical Rev. in Solid State and Materials Sciences,* 18 (3): (1993) 261.

37. M. A. Green, *Solar Cells, Operating principles, Technology and System applications,* Prentice-Hall, New Jersy, 1982.

38. W. Bantikassegn, P. Dannetun, O. Inganas and W. R. Salaneck, *Thin Solid Films,* 224 (1993) 232-236.